Energy Geoscience 2 (2021) 254–273

Contents lists available at ScienceDirect

Energy Geoscience

journal homepage: www.keaipublishing.com/en/journals/energy-geoscience

The role of the Mid-Cimmerian Unconformity on the quality of the underlying Skagerrak sandstone reservoir in the Kittiwake Field, central North Sea

Abdulati Araibi [a, *], Dorrik Stow [b], Helen Lever [b], Zeinab Smillie [b]

[a] Department of Earth Science, Elmergib University, Alkhoms, Libya
[b] Institute of Geo-Energy Engineering, School of Energy, Geoscience, Infrastructure and Society, Edinburgh, UK

ARTICLE INFO

Article history:
Received 21 April 2021
Received in revised form
22 July 2021
Accepted 28 July 2021

Keywords:
North sea
Kittiwake field
Unconformity
Skagerrak sandstone

ABSTRACT

The central aim of this paper is to address the role of unconformities in affecting reservoir quality. Do they facilitate diagenesis that leads to either enhanced or reduced porosity through dissolution or cementation? Or, do they have little effect? We have investigated the Late Triassic Skagerrak sandstone reservoir underlying the Mid-Cimmerian Unconformity in the Kittiwake Field, central North Sea. There is strong evidence for the development of secondary porosity through the dissolution of unstable silicate minerals, primarily feldspars. This includes the presence of oversized pores, partial dissolution of framework grains, and complete dissolution of grains leaving remnant grain margins and partially filled cores. This dissolution as a late-stage event is demonstrated by the complete lack of compaction effects on the secondary pores and diagenetic products despite present burial depths in excess of 3000 m. These observations, coupled with an absence of systematic trends linked to the unconformity surface in respects of reservoir porosity, feldspar amount and dissolution, and kaolinization, lead to the conclusion that there has been no effect of the Mid-Cimmerian Unconformity on reservoir quality in the Kittiwake Field. There is no evidence for leaching or cementation linked to meteoric water influx either shortly after deposition or following the uplift and exposure, which led to development of the Mid-Cimmerian Unconformity. Instead, we propose that the late-stage dissolution of feldspar and generation of secondary porosity are most likely related to the influx of organic acids and carbon dioxide generated either from thermogenic maturation of the source rock or from biodegradation of oil within the reservoir near the oil-water contact (OWC) transition zone.

1. Introduction

The effect of unconformities on reservoir quality has long been a matter of controversy. Several studies have been published suggesting a profound relationship exists between the presence of unconformity surfaces and reservoir quality (Ketzer et al., 2009; Shanmugam, 1990). By contrast, others have indicated that no such relationship exists (Ehrenberg and Jakobsen, 2001; Bjorkum et al., 1990). The existence and nature of any such relationship is significant for exploration geologists who might wish to target a potential hydrocarbon play beneath an unconformity surface. It is also important for reservoir sedimentologists in their assessment of reservoir quality above or below unconformities that occur within a known reservoir succession.

Authors who support the existence of such a relationship claim that many unconformities associated with stratigraphic traps have been found around the world, and there is a relationship between the producing reservoir formations and these unconformities (Shanmugam et al., 1988). They suggest that unconformities are not just a representation of sea level change or global tectonic events but also can cause diagenetic changes in the older sediments and control the distribution of the reservoir in different ways by

* Corresponding author.
E-mail address: aaraibi@elmergib.edu.ly (A. Araibi).

Production and Hosting by Elsevier on behalf of KeAi

https://doi.org/10.1016/j.engeos.2021.07.003

different geological processes. The diagenetic processes associated with the creation of the unconformities may either enhance porosity and permeability or enhance cementation (Rittenhouse, 1972), therefore creating either a high or low permeability zone, respectively, near the unconformity surface. Which of these processes occurs will therefore have a significant effect on reservoir quality.

Furthermore, it has been proposed that the structure and characteristics of these unconformities may also play a significant role in the processes of hydrocarbon migration and accumulation. They may work as a seal zone or traps in the areas of hydrocarbon accumulation where they are highly cemented, or they may act as pathways for fluid flow when they are associated with high permeability layers (Wu et al., 2013).

In contrast, other authors argue against the existence of such a relationship saying that there is no marked evidence for such a relationship and that any such effects could be a localised phenomenon (Bjorkum et al., 1990). These authors suggest that, even if erosion took place over a million to a few millions of years, the erosion rate would be expected to be a few tens to hundreds of metres and the rate of erosion would be greater than the rate of propagation of dissolution. Therefore, the sedimentary rocks below the unconformity surfaces would not be expected to preserve a distinct diagenetic change related to the creation of the unconformity. Furthermore, the absence of a systematic increase in the dissolution of feldspar grains towards the Cimmerian Unconformity within the Middle Jurassic Brent Group in the North Sea has previously been recognised by Ehrenberg and Jakobsen (2001). These authors documented that the dissolution of feldspar grains within the Brent Group sandstones in the Gulfaks Field is most likely to be related to the biodegradation of oil and not related to the influx of meteoric water through the unconformity surface.

The aim of this paper is to examine both hypotheses by investigating the effects of the Mid-Cimmerian Unconformity on the quality of the underlying sandstone reservoir of the Late Triassic Skagerrak Formation in the Kittiwake Field, central North Sea. The unconformity in this field has been selected for study because it juxtaposes relatively similar fine-grained sandstone facies either side of the unconformity surface. Any effect of the unconformity on reservoir quality should therefore be due to the presence of the unconformity itself rather than to a marked change in facies type. We do note that there has been a change from fluvial to shallow marine depositional environment across the unconformity. The potential effects of exposure and marine flooding will be discussed.

2. Geological setting

The Kittiwake Field is located approximately 100 miles ENE of Aberdeen in the western platform area of the central North Sea (Fig. 1). This field, which involves both stratigraphic and structural trapping, forms an east-west-trending elongated dome-shaped feature (Fig. 1) (Glennie 1998). The Upper Jurassic Fulmar Formation in this field unconformably overlies the Triassic Skagerrak Formation; the formations are separated by the Mid-Cimmerian Unconformity (MCU). In this study, the main target will be the Skagerrak Formation, which lies directly below the Mid-Cimmerian Unconformity. Therefore, any possible diagenetic effects related to this unconformity would be expected to be observed in this formation.

The main reservoir formations in the Kittiwake Field are the Fulmar and Skagerrak Formations; both formations occur at a depth of about 10000 ft (3050 m) TVSS. The Skagerrak Formation is underlain by the Upper Permian Zechstein halite, and the Fulmar Formation is overlain by Late Jurassic Kimmeridge Clay and Cretaceous sediments (Fig. 1). The deposition of the Skagerrak Formation, preservation of the Fulmar Formation and the creation of the structural aspects of the Kittiwake trap are controlled mainly by the diapiric movement of the underlying Zechstein halite (Glennie and Armstrong 1991).

3. Samples and methods

In this study, sedimentological and petrographic analyses are the two main approaches used. Samples and data were taken from 4 wells located in the Kittiwake Field, representing the entire thickness of the Skagerrak Formation. As the wells were originally drilled and recorded using imperial units (feet), we have necessarily retained these in the text and figures. Their metric equivalent is provided in parenthesis.

Sedimentological description (core logging) was carried out on more than 70 feet (21 m) of core from each of the Wells 21/18-2A, 21/18-3, 21/18-4 and 21/18-6. Description started with determination of grain size by visual comparison of core samples, using the Wentworth size classification scale. After the determination of grain sizes, the lithology and sedimentary structures were described for each well. The total described core length was approximately 372 feet (113 m).

The petrographic analysis has been performed mainly by (a) optical microscopy using transmitted light (plane and polarised), and (b) scanning electron microscopy (SEM), including normal and back-scatter electron (BSE) imagery. This is supported by limited X-ray diffraction (XRD) results from previous studies, where appropriate.

Thin-section petrographic analysis was used to identify the lithological texture, mineralogy, porosity and classification of sandstones. A total of 41 thin-sections, impregnated with blue epoxy resin in order to identify the pore space easily, were examined. Each sample was point-counted with 300 points per thin-section to maintain consistency and quantify the main sandstones texture and composition. The point counting result of each sample was then reported in a table as percentages of bulk volume, and transferred to an excel sheet in order to be used for sandstone classification diagram and to generate porosity and mineral distribution diagrams. This methodology is considered fully adequate and with sufficient scientific accuracy for the *comparative* quantification of mineralogy and porosity required for this study.

A further 19 thin-sections were prepared through milling and investigated using SEM. This technique allowed clearer observation of porosity, diagenesis and mineralogical distribution in the sandstones (Buckman, 2014). It was particularly useful in recognising the authigenic clay minerals (particularly kaolinite) from the detrital clay minerals as well as any possible diagenetic processes.

4. Sedimentological analysis results

4.1. Reservoir formations

The logged sections of each of the four wells are dominated by sandstone facies in the reservoir interval (Fig. 2). Our observations concur with previous work on the Kittiwake Field (Glennie and Armstrong, 1991), and enable the subdivision of the sections into two different formations in terms of sedimentary structures and the inferred depositional environment. These formations are separated by an erosional unconformity.

The upper sandstone unit is part of the Upper Jurassic Fulmar Formation, and represents a good reservoir interval. It consists of very fine to fine-grained sandstone, generally argillaceous or carbonate cemented, and moderately bioturbated. It is poor to moderately sorted and varies from light to dark grey and brownish grey in colour. It was deposited in shallow, low to moderately high-

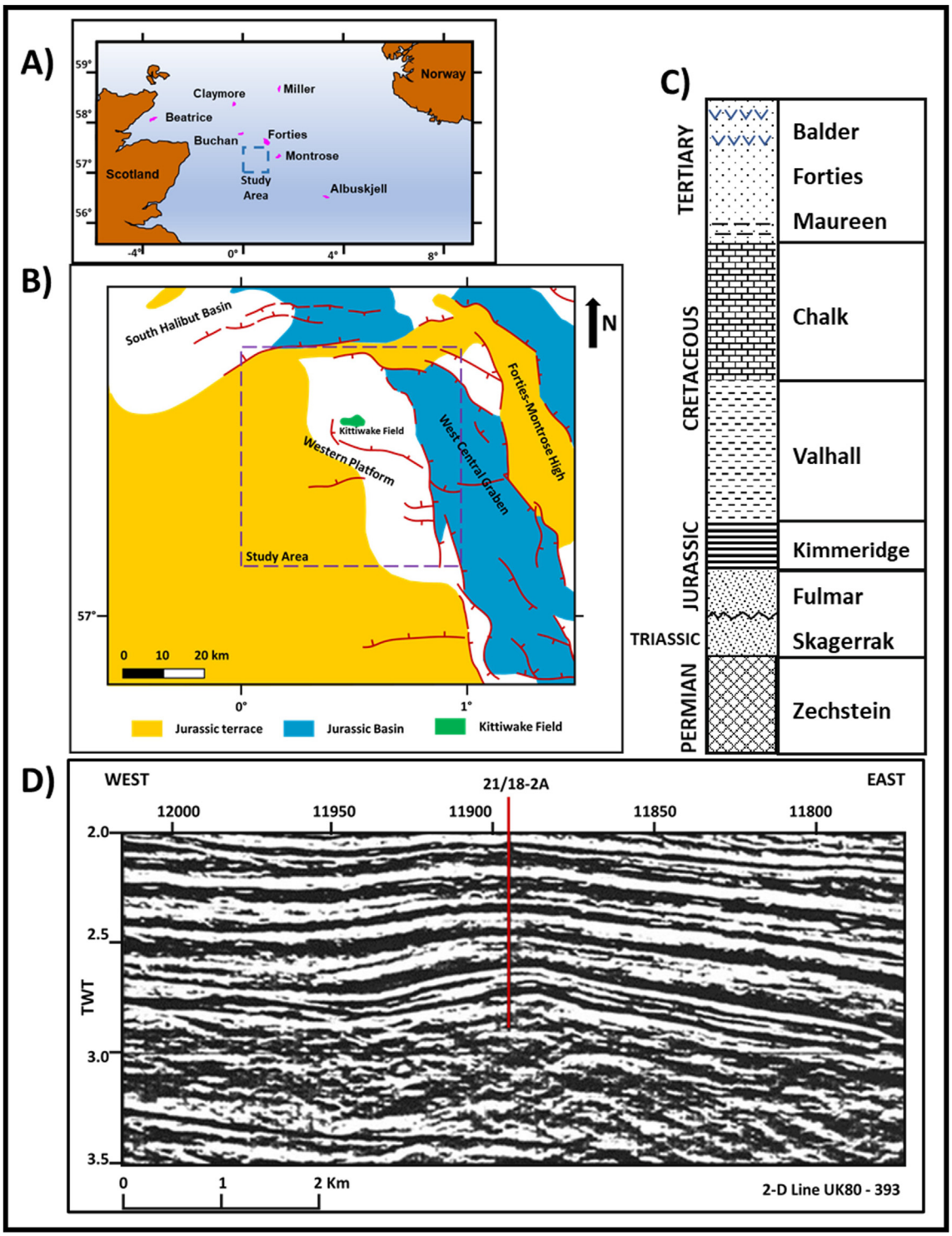

Fig. 1. Location of the Kittiwake Field in the central North Sea (after Wakefield et al., 1993), and detail of stratigraphic column for this part of the North Sea. Seismic line through the discovery Well 21/18-2A of Kittiwake Field (from Glennie and Armstrong 1991).

energy, storm-influenced marine environments (Glennie and Armstrong, 1991).

The lower sandstone unit is part of the Upper Triassic Skagerrak Formation, and also represents a good reservoir interval. It consists mainly of very fine to fine-grained sandstone; the sandstones are generally laminated, moderately or poorly sorted and vary from light to medium grey in colour and become more red coloured with depth. The formation can be divided into two facies associations identified in the Kittiwake Field, which are sheet-flood and overbank sediments (Glennie and Armstrong, 1991). The Skagerrak Formation, lying directly beneath the Mid-Cimmerian Unconformity, is the main target of the petrological study, as presented in the following sections.

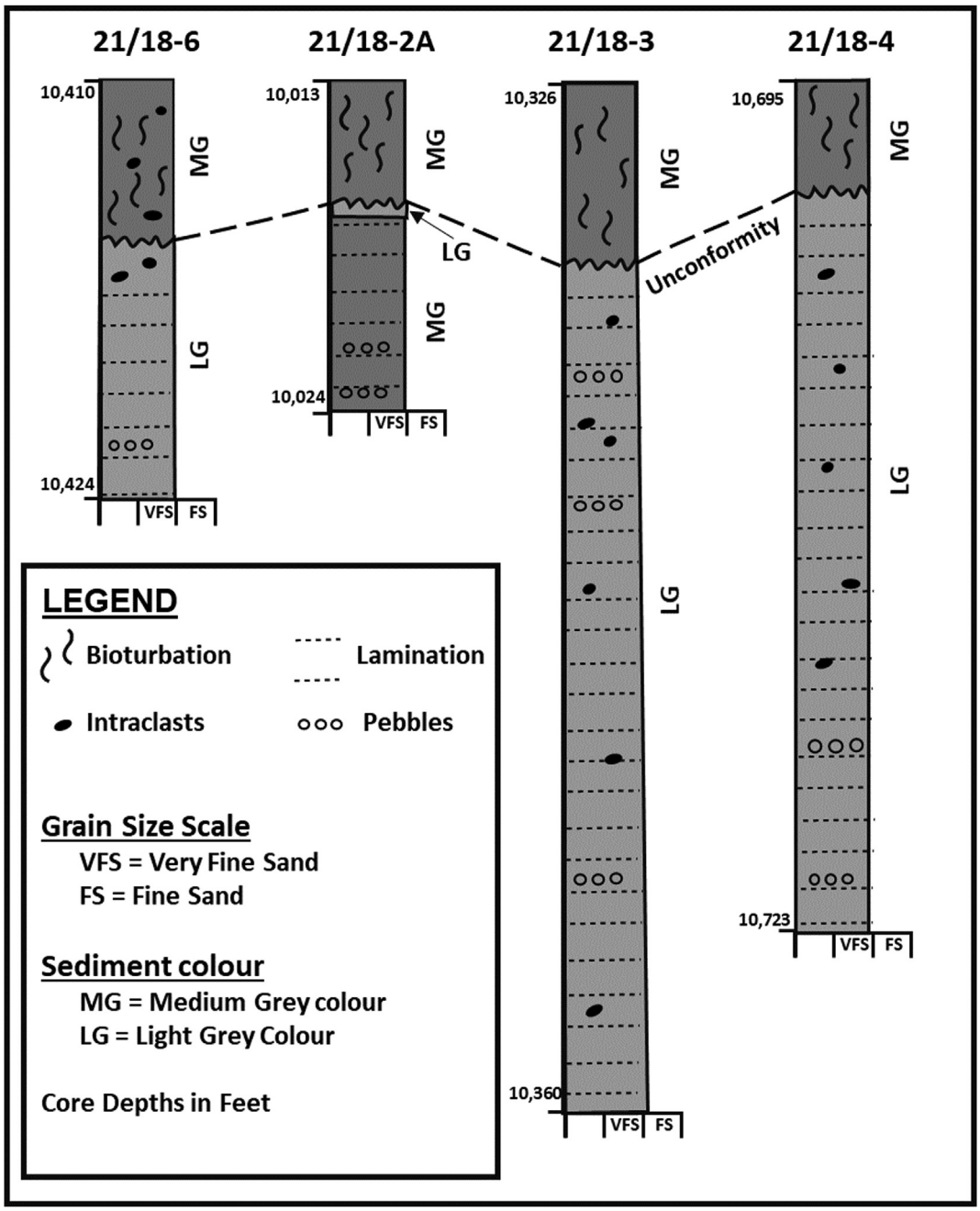

Fig. 2. Sedimentological core descriptions of the four study wells from the Kittiwake Field. The figure illustrates the principal facies characteristics, subtle differences between the Fulmar and Skagerrak Formations, and the location of the Mid-Cimmerian Unconformity, which separates the Triassic Skagerrak Formation from the Upper Jurassic Fulmar Formation.

4.2. Facies and texture

Three sandstone facies can be identified in the Skagerrak Formation based on the grain size: facies 1, 2 and 3. This facies distinction is very subtle as all three facies range in grain size from very fine to fine sand.

Facies 1 is very fine-grained, poorly to moderately sorted sandstone. Detrital grains are mainly sub-angular to sub-rounded, and the grain contacts indicate a limited amount of compaction. This is supported by the presence of some lithic clasts and contorted flakes of mica. It is generally bioturbated, less commonly with indistinct wavy lamination, and light to dark grey in colour. This facies is the dominant facies in Well 21/18-6, and interbedded with Facies 2 in Wells 21/18-2A and 21/18-3.

Facies 2 is very fine to fine-grained, poorly to moderately sorted sandstone. Detrital grains are mainly sub-angular to sub-rounded, and there is clear evidence of compaction. Lithic clasts and carbonaceous clasts are present in some parts. Parallel and wavy lamination is common, and bioturbation is rare. It ranges from grey to reddish-brown in colour. This is common in Wells 21/18-2A, 21/18-3 and 21/18-4, more typically in the Skagerrak Formation.

Facies 3 is fine-grained, poorly to moderately sorted sandstone. Detrital grains are mainly sub-angular to sub-rounded, and there is clear evidence of compaction. Lithic clasts and carbonaceous are

rare. Parallel and wavy lamination is common and bioturbation is rare. It ranges from grey to reddish-brown in colour. It mostly occurs in Well 21/18-4.

4.3. Sandstone classification

Petrographic classification of sandstone types identified from the 41 thin-sections studied is shown in Fig. 3, and the data is presented in Tables 1–4. As the main framework grains are quartz, feldspar and rock fragments, the results are plotted using classification scheme (in which polycrystalline quartz is counted as rock fragments. Most of the Skagerrak Formation sandstones are classified as arkosic to subarkosic, comprising mainly of quartz, feldspar and granitic rock fragments. A small number of sandstone samples are classified as lithic arkose to lithic subarkose, as a result of their higher rock fragment content, and one sample falls into the feldspar litharenite category, due to its high rock fragment content (24%, Well 21/18-4, depth 10698.5 ft (3260.9 m)). Most of the very fine to fine sandstone facies are distributed between arkose and subarkose, whereas the coarser sandstone facies (i.e. fine-grained sandstones) are mainly lithic arkose to lithic subarkose. The trend of increasing rock fragments and polycrystalline quartz with increasing grain size is typical for terrigenous sediments in general (Pettijohn et al., 1972).

4.4. Mineralogy

This section describes in detail the main composition of the studied Skagerrak sandstones based on the point counting results of the 41 studied samples (Tables 1–4).

4.4.1. Framework minerals

Quartz: The principal framework grain in all samples is monocrystalline quartz. Quartz content ranges from 17% to 55%. Some quartz grains contain abundant mineral inclusions, and others show cracked and corroded quartz grains with precipitation (inclusion) of mica (Fig. 4 A). Sutured boundaries between quartz grains are present in some samples, which indicate some significant compaction has occurred (Fig. 4 B).

Feldspar: The second most common framework grain in all but one sample is feldspar. Although distinction between feldspar types is difficult, we infer, on the basis of observed morphology and twinning characteristics, that the majority are potassium feldspar, with lesser amounts of plagioclase and microcline feldspars. Feldspar content ranges from 5% to 20%. Most of the observed feldspar grains exhibit variable degrees of alteration, replacement and in many cases partial or complete dissolution. Some feldspar grains, presumably originally calcium plagioclase, have been replaced partially or completely by authigenic calcite (Fig. 4C). Other feldspar grains were partially dissolved and re-filled with authigenic clay (Fig. 4 D). In some cases, and within the same field of view, there are intact feldspar grains, partially dissolved grains and completely dissolved grains, yielding good secondary porosity. Some of these dissolved grains have been partially or completely replaced by precipitation of kaolinite, which creates microporosity (Fig. 4 E).

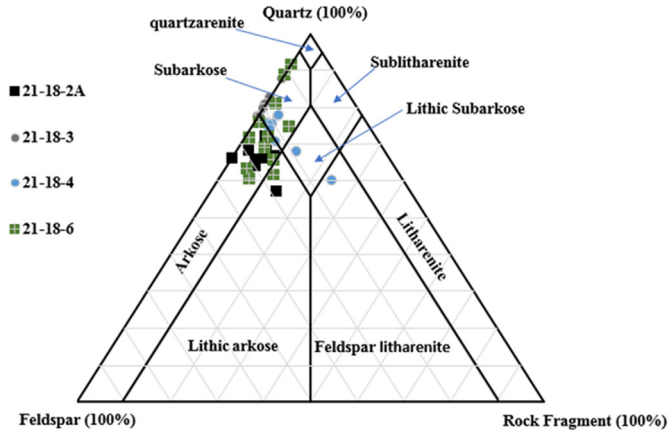

Fig. 3. Classification of the Skagerrak Formation sandstones according to the Quartz-Feldspar-Lithic triangular plot modified from Pettijohn et al. (1972).

Rock fragments: Rock fragment content ranges from 0% to 16% (mostly < 5%). Polycrystalline quartz grains are the most common rock fragments in most facies within the Skagerrak Formation. Other rock fragments include shale clasts and clay intraclasts or pebbles (Fig. 4F). Some of these fragments have been altered and oxidized.

4.4.2. Accessory minerals

Mica: Although being considered as an 'accessory' mineral, mica is in fact common to very common in most of the studied samples, ranging from 0% to 24.7% (typically > 5%). Both muscovite and biotite are present, muscovite the more dominant. Both types occur as distinctive thin, elongate flakes that lie parallel to the bedding and lamination planes and have become deformed and compacted between framework grains (Fig. 5A). There is marked variation in the distribution and content of mica between facies in the area of study, where some samples are highly micaceous and others contain less than 2% mica. This variation appears to be proportional to grain size, which can be related to the depositional process rather than to the provenance: the finer the grain size the more abundant the mica.

Iron oxides and pyrite: Iron oxides are rare to common in all samples studied, ranging from 1.3% to 8.4% (typically 2%–5%). These grains likely include both detrital and authigenic types. Pyrite is less common, and occurs sporadically as clusters of black cubic grains within pores or in association with clays (Fig. 5B) and as dense nodules, framboids, or in amorphous form in some other samples. Alteration of pyrite to iron oxide may have occurred during uplift and exposure and appears as a red colouration along the edge of the pyrite grains (Fig. 5C).

4.4.3. Authigenic minerals

Calcite cement: Half of the studied samples contain authigenic calcite cement, ranging from 1.6% to 12.3%, with the exception of one sample in Well 21/18-2A, which contains about 18% calcite cement. The other samples have no recorded calcite. The calcite occurs in different forms – intergranular, euhedral and as replacement of feldspar grains (Fig. 5 D). Fig. 5 E shows poikilotopic calcite that has filled the pore space after a partial or complete grain dissolution as it squeezed between grains; this example shows the high birefringence and relief of calcite compared to the quartz grains. Fig. 5F shows partly dissolved plagioclase filled by calcite. Another type of calcite was observed as well; this calcite seems to have been precipitated in a late stage and may have formed mainly due to the replacement of feldspar grains.

Two main types of calcite are identified and inferred to represent two phases of precipitation:

(a) Early calcite cement: poikilotopic and intergranular calcite cement can be interpreted as exhibiting an early diagenetic process which may support the other detrital framework grains and prevent later diagenesis processes (Fig. 5 E).
(b) Late calcite cement: calcite that has been formed by alteration and replacement of feldspar grains or that has filled

Table 1
Petrographic analysis data for Well 21/18-6.

Sample No.	Core Depth (ft)	Facies	CONSTITUENT (%)								Total %
			Porosity %	Framework Minerals			Accessory Minerals	Cement		Others	
				Quartz	Feldspar	Rock Fragment	Mica	Calcite	Clay	Iron Oxide	
24	10414.7	1	10	55	5	0	2	0	20	8	100
25	10415.7	1	14.9	44.7	9.3	1	2.8	0	24.3	3	100
26	10415.8	1	13.3	50	6.3	0	2.3	0	23.4	4.7	100
27	10417	1	13.6	44.7	10.3	4.7	5	0	19.3	2.4	100
28	10418.7	1	11.6	41.7	13.3	2.7	2	5	21	2.7	100
29	10420.2	1	8.4	41	15.5	0.5	2.1	0	29.9	2.6	100
30	10424	1	9	45.1	13.6	0.5	1.6	1.6	25.6	3	100
1-B1	10431.2	1	9.1	37.5	20.3	4.1	1	5.6	13.6	8.8	100
2/B2	10437.3	2	2.3	36.3	13.3	3	16.7	4	20.6	3.8	100
3/B2	10449.4	1	7.7	45.4	17.3	6.3	2.1	5.2	11.7	4.2	100
4/B2	10459.5	1	6	40	17.7	7.3	2.3	6.2	16.4	4	100
5/B2	10468	1	4.6	41	20.7	3	1	9	18	2.7	100

Table 2
Petrographic analysis data for Well 21/18-2A.

Sample No.	Core Depth (ft)	Facies	CONSTITUENT (%)								Total %
			Porosity %	Framework Minerals			Accessory Minerals	Cement		Others	
				Quartz	Feldspar	Rock Fragment	Mica	Calcite	Clay	Iron Oxide	
50	10014.8	1	5	52	10	0	5	0	25	3	100
51	10016.8	1	10	45	17	0	0	0	25	3	100
53	10017.1	2	1.3	17	8.6	0	12	0	57.5	3.6	100
54	10017.5	1	4	38	16.6	3	5.6	0	28.3	4.5	100
55	10021	1	6.3	30	15	7.4	6	0	30.3	5	100
56	10023	1	7.8	38.1	16.3	1.4	8.9	0	25.4	2.1	100
23/B2	10026.5	2	3.4	40	13	2.3	13	0	23.3	5	100
24/B2	10033.75	2	2.3	36.4	13.3	4.7	16	0	23.3	4	100
25/B2	10053.9	1	1.3	38.3	13.4	3	4.3	18	19.2	2.5	100
26/B2	10076.9	2	6	35.3	16.3	3.3	8	3	25.6	2.5	100
27/B2	10111	1	7	33.9	13.6	3.6	3.3	3	29.3	6.3	100

Table 3
Petrographic analysis data for Well 21/18-3.

Sample No.	Core Depth (ft)	Facies	CONSTITUENT (%)								Total %
			Porosity %	Framework Minerals			Accessory Minerals	Cement		Others	
				Quartz	Feldspar	Rock Fragment	Mica	Calcite	Clay	Iron Oxide	
6/B2	10332	1	5	38.7	9.1	2.1	8.1	11.4	19.8	5.8	100
7/B2	10332.5	1	2	42.3	12.3	0	7.8	0	32.3	3.3	100
8/B2	10333.5	2	2.3	36.3	7.7	0	24	0	25	4.7	100
9/B2	10336.5	1	1.3	43.9	12.5	0.2	10.4	0	28.4	3.3	100
10/B2	10343.8	2	1	36	8.7	0	17	0	33.3	4	100
11/B2	10352.8	2	1	36	5	0	15	4	37	2	100
12/B2	10361	2	3.8	40	9.5	0	12	0	26.3	8.4	100
13/B2	10377.8	2	6.7	38	9.7	0	13.3	4.3	26.7	1.3	100

Table 4
Petrographic analysis data for Well 21/18-4.

Sample No.	Core Depth (ft)	Facies	CONSTITUENT (%)								Total %
			Porosity %	Framework Minerals			Accessory Minerals	Cement		Others	
				Quartz	Feldspar	Rock Fragment	Mica	Calcite	Clay	Iron Oxide	
14/B2	10698.5	1	4	39	10	16	3	0	23	5	100
15/B2	10698.7	2	2.7	40.7	9.3	2.3	8.3	0	33	3.7	100
16/B2	10700.5	3	4.3	28	8	1.3	24.7	7.3	21.4	5	100
17/B2	10701.8	2	5	35.5	10	1.3	6	12.3	27.3	2.6	100
18/B2	10708.5	3	1.7	27	7.8	1	24.4	11.4	24.4	2.3	100
19/B2	10714.5	2	1.3	38.3	12	4	3.7	11	25	4.7	100
20/B2	10724.5	2	7	36.7	10	2	8	4.3	24	8	100
21/B2	10734.1	2	3.8	38.7	11.3	2.3	5.3	7.3	27.3	4	100
22/B2	10746.5	2	7	38.3	10.7	7.3	3	5	25.4	3.3	100

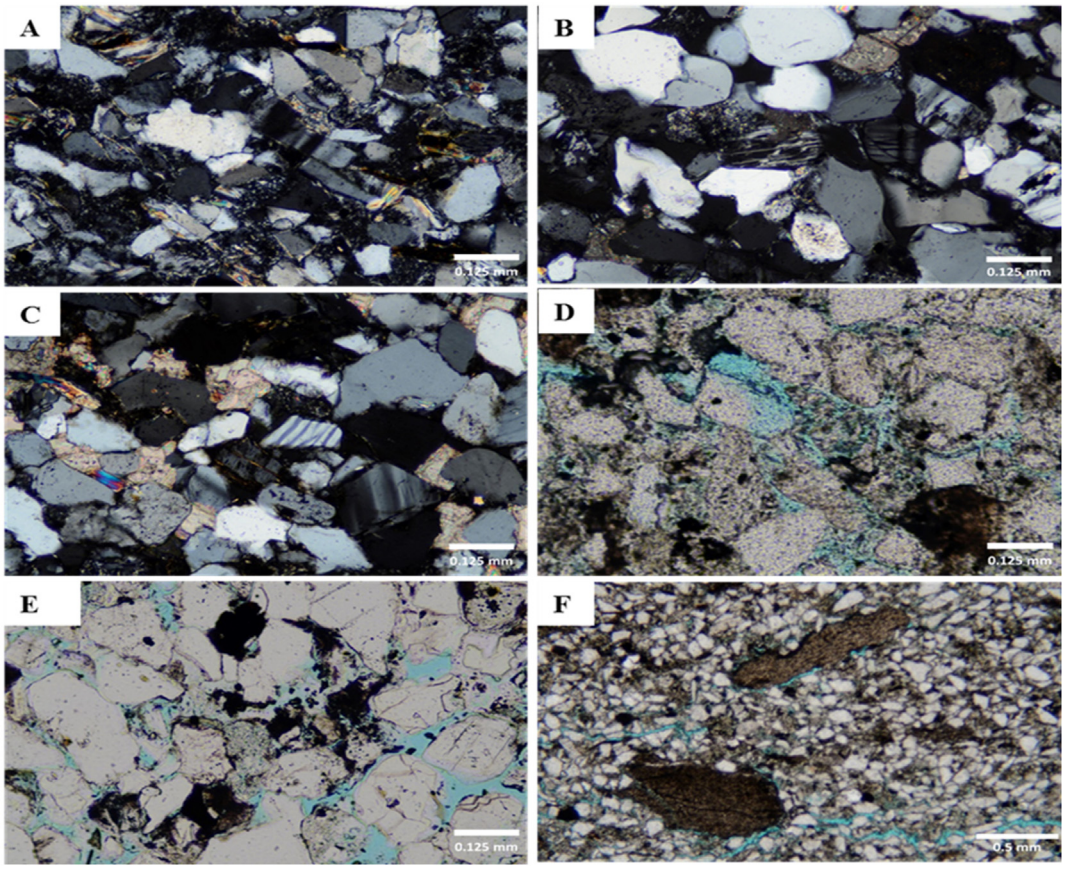

Fig. 4. Thin-section photomicrographs showing different petrographic features. **A.** Typical view of very fine to fine-grained sandstone facies showing corroded quartz grains with precipitation (inclusion) of mica in some cases: Well 21/18-4, 10698.75 ft (3261 m). **B.** Typical view of very fine to fine-grained sandstone facies showing signs of compaction represented by the sutured boundaries between quartz grains: Well 21/18-6, 10449.4 ft (3184.9 m). **C**. Detailed view showing partial and complete dissolution of calcareous feldspar grain to be replaced by authigenic calcite: 21/18-2A, 10053.9 ft (3064.4 m). **D**. Typical view of feldspar grains with inclusion filled with clay: Well 21/18-6, 10424 ft (3177.2 m). **E**. Detailed view of polished thin-section showing some dissolved feldspar grains which have been followed or replaced by precipitation of kaolinite and formation of microporosity: Well 21/18-6,10417 ft (3175.1 m). **F**. Typical view of fine grained sandstone facies showing shale fragments and clay intraclasts or pebbles of clay: Well 21/18-2A, 10021 ft (3054.4 m).

dissolution pores indicates that this cementation was formed later and post-dates the dissolution process (Fig. 5 F).

Clay minerals: Whereas some of the clay minerals present are undoubtedly authigenic, others are most likely of detrital origin. They are therefore documented separately below.

4.4.4. Clay minerals

The Skagerrak sandstones are clay-rich, ranging from 19% to 37%, with one sample having 57.5% clays and so perhaps more properly classified as a sandy mudstone.

Kaolinite: Kaolinite is one of the main clay minerals found in Skagerrak sandstones. It is present in two distinct forms: irregular, poorly-developed crystals in association with altered detrital mica flakes (Fig. 6 A), and more regular crystals or pseudohexagonal plates stacked in booklets (Fig. 6 B). The latter are more common and many are found occupying intergranular pores or within secondary pores that may have been formed by dissolution of feldspar grains.

Chlorite: Chlorite is also common, and typically found as a clay coating over other grains. The structural pattern of the observed chlorite grain coating is complex and in some cases seems to be associated with other clay types (e.g. illite or smectite). Chlorite grain coats may have been formed during early to medium diagenetic phases as a result of replacement of other clay minerals such as smectite and kaolinite or due to dissolution and re-precipitation of detrital chlorite. The presence of such authigenic cements in Skagerrak sandstones may have played a significant role in limiting other types of cementation (e.g. quartz cementation) (Stricker and Jones, 2016). In many cases, partly or completely dissolved feldspar grains are observed being coated by chlorite, preserving the original shape of the feldspar grains from any further diagenetic effects. This clearly indicates that the chlorite grain coating was most likely to have occurred prior the dissolution of feldspar grains.

4.5. Types of porosity

Three main types of porosity can be identified within the Skagerrak sandstones: intergranular porosity, intragranular porosity (grain dissolution porosity) and microporosity. In addition, there is some fracture porosity and circum-granular porosity noted. The visible point counted porosity is relatively low to moderate, ranging from 1% to 15% (Table 5). This includes both primary and secondary porosity. This compares with rather higher measured core data from helium porosimetry, which show 3% to 21% porosity. Clearly, the point counting technique has missed some porosity – most likely some of the microporosity. In addition, the core depth of samples taken for this study is not exactly the same as the depths of those used for core analysis measurements.

4.5.1. Macroporosity

Only a low proportion of the macroporosity is identified as

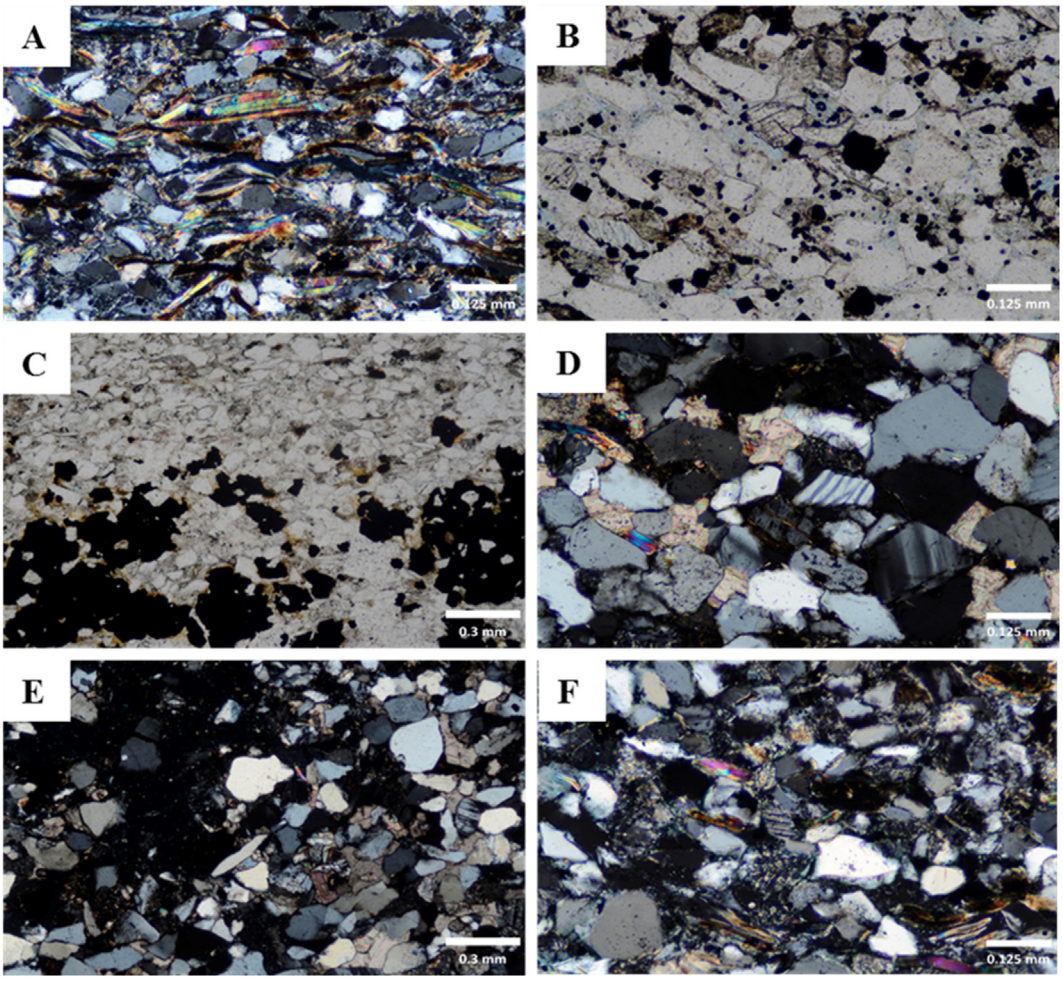

Fig. 5. Thin-section photomicrographs of some authigenic and accessory minerals. **A**. showing distinctive flakes of mica compacted and deformed between detrital grains. Well 21/18-4, 10700.5 ft (3265.1 m). **B**. showing clusters of black cubic pyrite within pores or in association with other clay. Well 21/18- 4, 10724.5 ft (3268.8 m). **C**. Typical view showing alteration of pyrite to iron oxide appearing as a red colouration along the edge of pyrite. Well 21/18-3, 10361 ft (3158 m). **D**. Detailed view showing partial and complete dissolution of calcareous feldspar grain to be replaced by authigenic calcite. Well 21/18-2A, 10053.9 ft (3064.4 m). **E**. View of poikilotopic calcite which has occupied the pore space. Well 21/18-6, 10468 ft (3190.6 m). **F**. Detailed view showing late precipitation of calcite due to the replacement of feldspar grains. Well 21/18-2A, 10053.9 ft (3064.4 m).

intergranular porosity (Fig. 6C); whereas most is intragranular porosity due to grain dissolution. This porosity has been interpreted as a secondary porosity formed due to the partial or complete dissolution of detrital grains (commonly feldspar), as their grain shape and outlines are still represented in places (Fig. 6 D). However, some of this secondary porosity has been subsequently refilled by precipitation of clay or calcite (Fig. 6 E). The macroporosity occurring as elongated fracture porosity and circumgranular porosity (developed around grains) (Fig. 6 F) may be resulted from pressure solution or due to load release during uplift. However, such porosity may also form as a result of poor sample preparation.

4.5.2. Microporosity

In the studied samples, these micropores were recognised under the petrographic microscope by the presence of very small specks of blue impregnating resin filling the micropores, and more easily from the SEM images. Two main types of micropores are noted: (a) within altered or leached detrital grains, most commonly within partially dissolved feldspar grains (Fig. 7 A) and/or in between the expanded flakes of mica (Fig. 7 B); and (b) associated with authigenic clays, mainly within kaolinite crystals (Fig. 7C and D). The SEM images confirmed that most of the observed micropores are associated with the authigenic clays (mainly within a mass of kaolinite crystals) and within the partially dissolved feldspar grains (Figs. 7 and 8).

5. Petrographic relationship to the Mid-Cimmerian Unconformity

Most of the previous studies which suggest that unconformities have a direct effect on the underlying sediments attribute this to the leaching of certain minerals due to the influx of meteoric water during uplift and erosion. To be able to test this hypothesis, it was necessary to study the pattern of vertical distribution of unstable minerals and the reservoir properties under the unconformity surface in the studied wells. The results of this are outlined below.

5.1. Feldspar

There is no significant systematic vertical variation (vertical trend) in the amount and distribution of feldspar below the unconformity in three of the four studied wells. However, in one well (Well 21/18-6), we do observe a fairly systematic decrease in feldspar toward the unconformity surface (Table 6), from 20% at 15 feet (4.572 m) below the unconformity surface to less than 5% very close

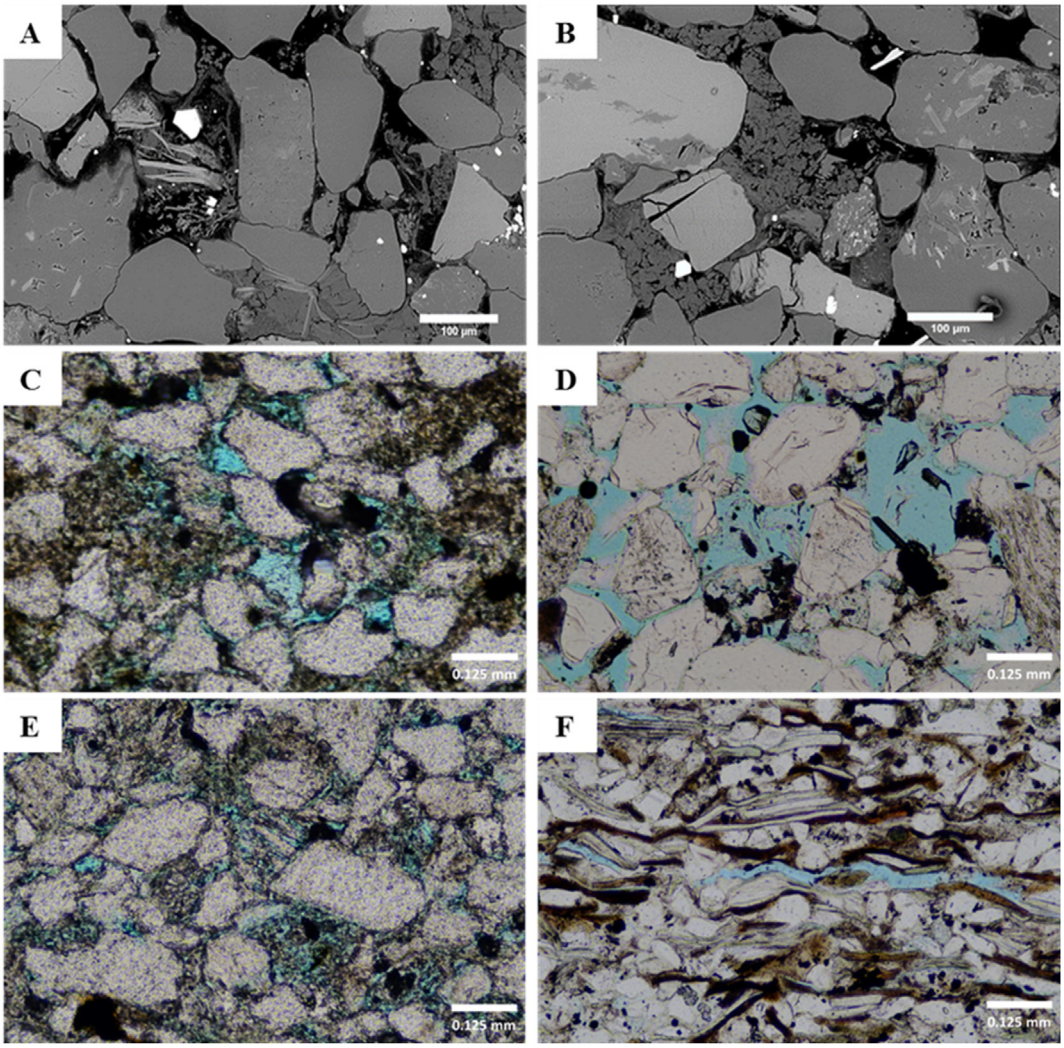

Fig. 6. Thin-section photomicrographs and backscattered electron (BSE) images showing: **A**. Kaolinite in association with altered detrital mica flakes. Well 21/18-6, 10417 ft (3175.1 m). **B**. Kaolinite in regular crystals or pseudohexagonal plates stacked in "booklets" (SEM image). **C**. Intergranular porosity which exists as pores between framework detrital grains. Well 21/18-2A, 54, 10017.5 ft (3053.3 m). **D**. Partial or complete dissolution of feldspar grain (the grain shape and outlines still represented), Well 21/18-6, 10417 ft (3175.1 m). **E**. Secondary pores refilled by precipitation of clay, Well 21/18-6, 10415.7 ft (3174.7 m). **F**. Elongated fracture porosity, Well 21/18-4, 10700.5 ft (3261.5 m).

Table 5
Petrographic analysis data of porosity content below the unconformity surface in Wells 21/18-6, 21/18-2A, 21/18-3 and 21/18-4.

Well 21/18-6		Well 21/18-2A		Well 21/18-3		Well 21/18-4	
MCU at 10415.5 ft		MCU at 10017 ft		MCU at 10332 ft		MCU at 10698.7 ft	
Depth (ft)	Porosity %	Depth (ft)	Porosity %	Depth (ft)	Porosity %	Depth (ft)	Porosity %
10415.7	14.9	10017.1	1.3	10332	5	10698.75	2.7
10415.8	13.3	10017.5	4	10332.5	2	10700.5	4.3
10417	13.6	10021	6.3	10333.5	2.3	10701.8	5
10418.7	11.6	10023	7.8	10336.5	1.3	10708.5	1.7
10420.2	8.4	10026.5	3.4	10343.8	1	10714.5	1.3
10424	9	10033.8	2.3	10352.8	1	10724.5	7
10431.2	9.1	10053.9	1.3	10361	3.8	10734.15	3.8
10437.3	2.3	10076.9	6	10377.8	6.7	10746.5	7
10449.4	7.7	10111	7				

to the unconformity (Fig. 9). This reduction is most likely due to the dissolution of the unstable feldspar grains; this can be either partial or complete dissolution. Evidence for such alteration and dissolution is common in all four wells (Fig. 8 A, B, C and D), although the systematic variation is only noted in the first 15 feet (4.572 m) of Well 21/18-6 (Fig. 9).

5.2. Kaolinite

Kaolinite is the most common clay mineral for all the studied wells in Skagerrak sandstones. In most samples, kaolinite occurs in association with feldspar alteration and dissolution, filling pore spaces (Fig. 7C and D), whereas in other cases it occurs in

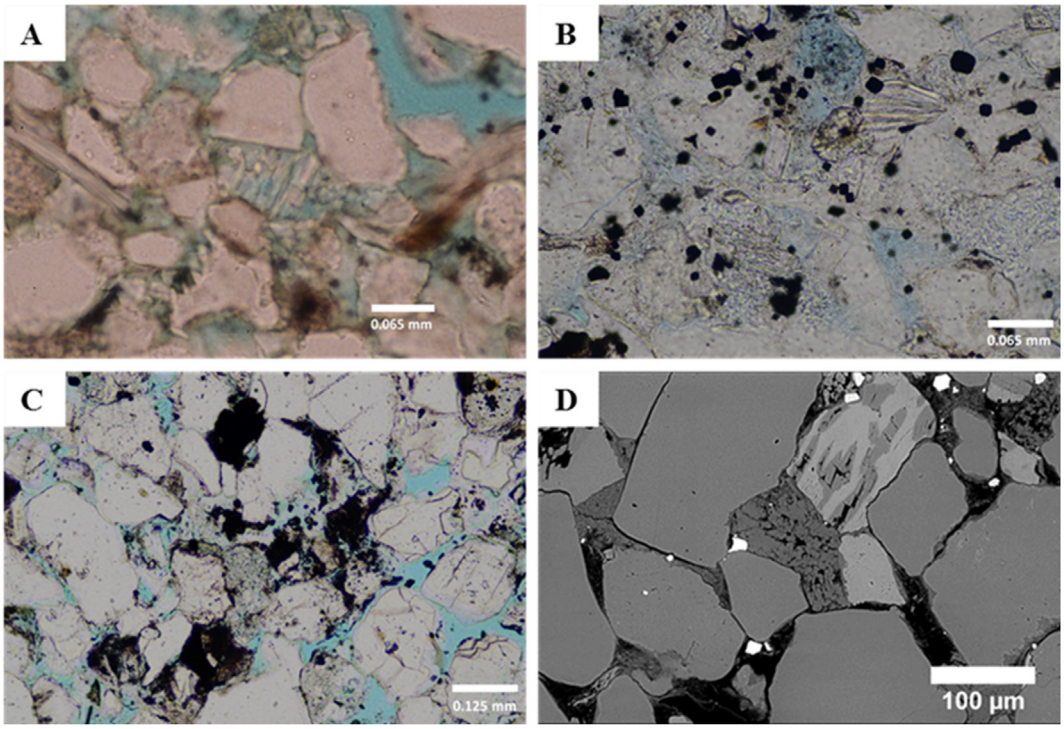

Fig. 7. Thin-section photomicrographs and backscattered electron images showing: **A**. Typical view of micropores within partially dissolved reservoir grains. Well 21/18-2A, 10023 ft (3055 m). **B**. Presence of micropores between the expanded flakes of mica. Well 21/18-4, 10724.5 ft (3268.8 m). **C**. Detailed view showing micropores associated with the authigenic clays. Well 21/18-6, 27, 10417 ft (3175.1 m). **D**. Microporous within mass of blocky kaolinite that was most likely to have been formed as result of feldspar alteration. Well 21/18-6. 10449.4 ft (3184.9 m).

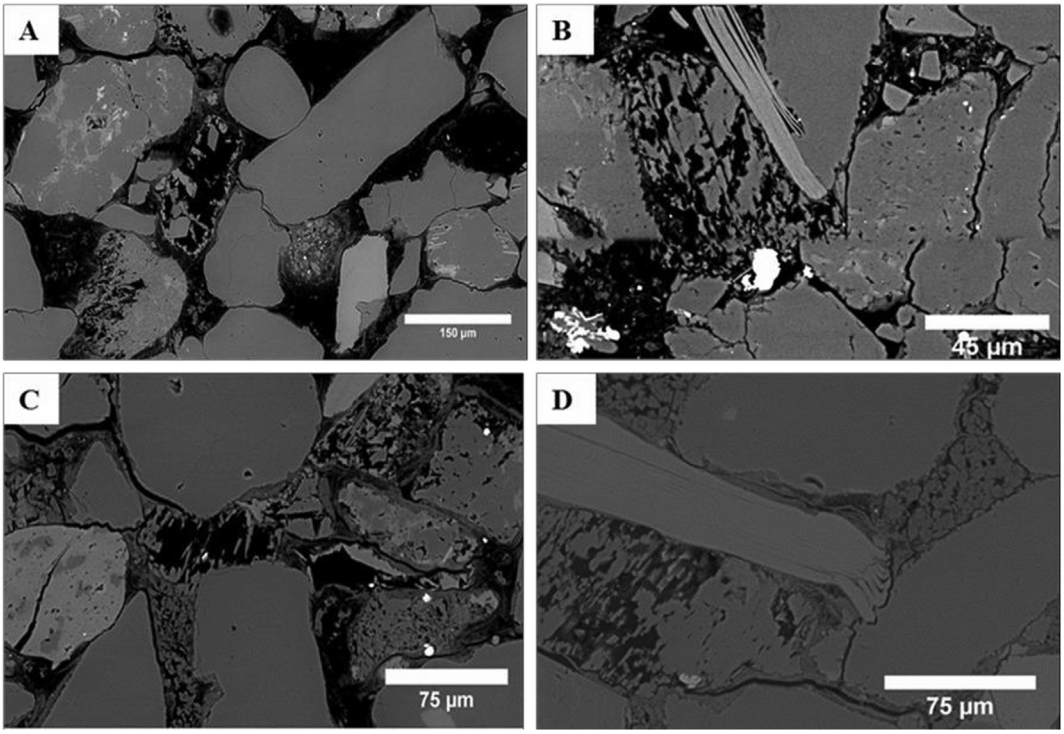

Fig. 8. BSE images showing evidence for the alteration and dissolution of feldspar grains within Skagerrak sandstone. A. Complete dissolution of feldspar grains located about 34 ft (10.36 m) below the unconformity surface in well 21/18-6, Depth: 10449.4 ft (3184.9 m). B. Partial dissolution of feldspar grains located just below the unconformity surface in Well 21/18-3, Depth: 10332 ft (3149.2 m). C. Partial dissolution of feldspar grains located about 0.5 ft (0.15 m) below the unconformity surface in well 21/18-2A, Depth: 10017.5 ft (3053.3 m). D. Dissolution of feldspar grains located about 15 ft (4.6 m) below the unconformity surface in well 21/18-4, Depth: 10714.5 ft (3265.8 m).

Table 6
Petrographic analysis data of feldspar content below the unconformity surface in Wells 21/18-6, 21/18-2A, 21/18-3 and 21/18-4.

Well 21/18-6		Well 21/18-2A		Well 21/18-3		Well 21/18-4	
MCU at 10415.5 ft		MCU at 10017 ft		MCU at 10332 ft		MCU at 10698.7 ft	
Depth (ft)	Feldspar %	Depth (ft)	Feldspar %	Depth (ft)	Feldspar %	Depth (ft)	Feldspar %
10415.7	9.3	10017.1	8.6	10332	9.1	10698.75	9.3
10415.8	6.3	10017.5	16.6	10332.5	12.3	10700.5	8
10417	10.3	10021	15	10333.5	7.7	10701.8	10
10418.7	13.3	10023	16.3	10336.5	12.5	10708.5	7.8
10420.2	15.5	10026.5	13	10343.8	8.7	10714.5	12
10424	13.6	10033.8	13.3	10352.8	5	10724.5	10
10431.2	20.3	10053.9	13.4	10361	9.5	10734.15	11.3
10437.3	13.3	10076.9	16.3	10377.8	9.7	10746.5	10.7
10449.4	17.3	10111	13.6				

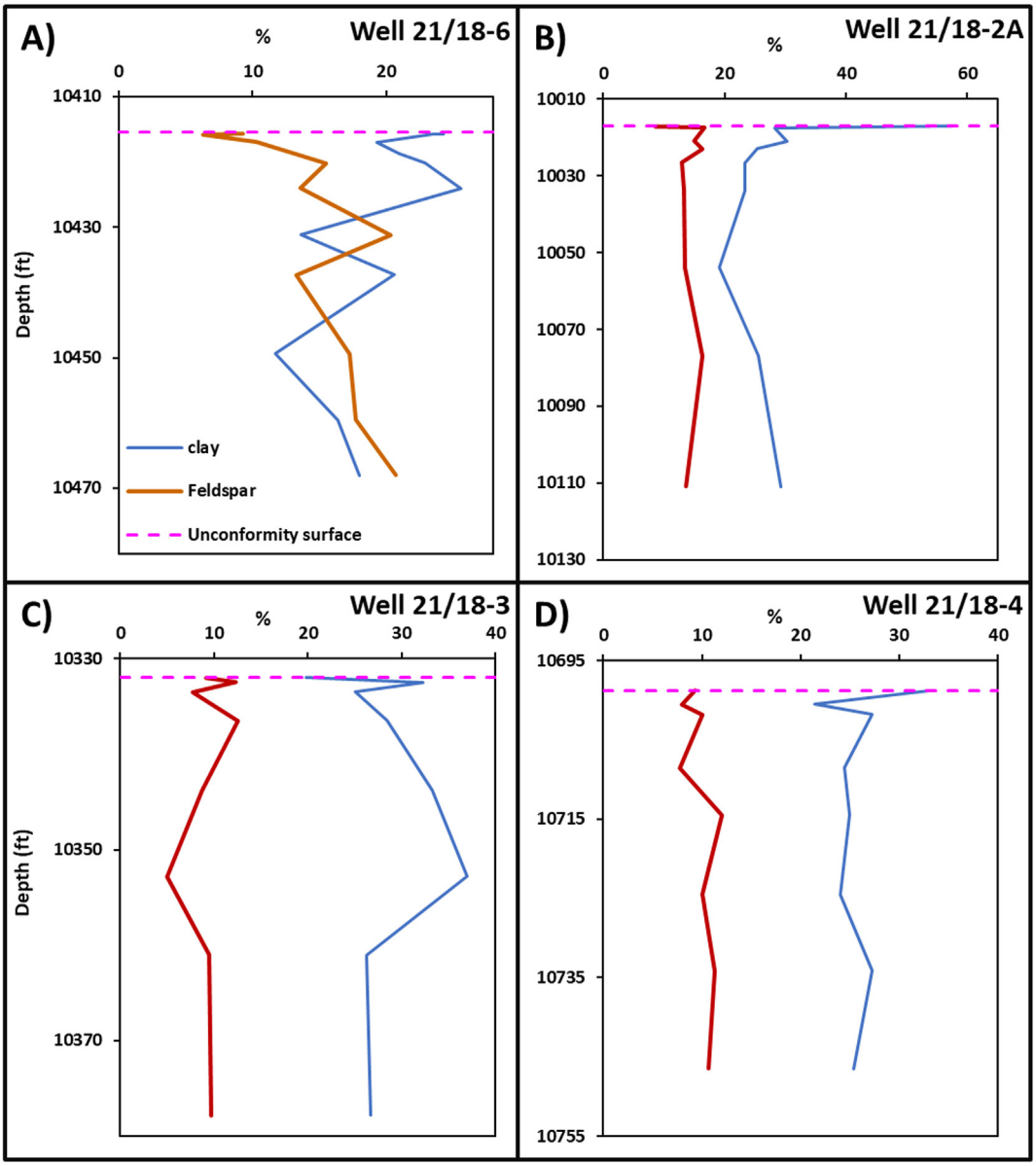

Fig. 9. The vertical distribution patterns of feldspar and clay minerals below the Mid-Cimmerian Unconformity in the studied wells. Note the systematic decrease in the feldspar amount toward the unconformity surface in Well 21/18-6 only. **B**, **C** and **D** show absence of vertical systematic distribution patterns of feldspars toward the unconformity surface in the Wells 21/18-2A, 21/18-3 and 21/18-4, respectively. There is no apparent systematic distribution of clay mineral content in relation to the unconformity. There is a lack of correlation between clay and feldspar below the unconformity surface, except in Well 21/18-6, which shows some positive correlation.

association with other clay minerals (e.g. smectite and illite) and detrital mica. In this case, the irregular grain shape and poorly developed crystallinity (Fig. 6 A) suggests a possible detrital origin. However, it is very difficult to differentiate between detrital and early authigenic kaolinite, especially within fine sandstones (Fig. 10 A).

In the majority of samples, however, the more regular grain shape, well-developed crystallinity and stacked booklets or vermicular habit, suggests a late diagenetic product formed in situ due to alteration and replacement of feldspar (Fig. 10 B and C). The latter, which is commonly recognised as a microporous mass of blocky kaolinite within pore space, is most likely to have been formed as a result of feldspar alteration and dissolution and usually appeared within a hint of the grain outline (Fig. 10 D). Although the evidence indicates that most of the observed kaolinite was formed in situ and related to later diagenetic processes (including euhedral booklets and high microporosity within kaolinite masses), some probable detrital kaolinite is also present. Therefore, the variations of kaolinite distribution below the Mid-Cimmerian Unconformity appear to be more complex than a direct relationship to feldspar mineral dissolution.

It proved difficult to quantitatively evaluate the amount and distribution of authigenic kaolinite in relation to the unconformity surface for two reasons: (a) it is not always easy to distinguish kaolinite from the other clay minerals; and (b) it is not always easy to distinguish authigenic from detrital kaolinite. However, because kaolinite is the main clay mineral type in the studied samples, we can use the total clay content as a proxy for kaolinite. The vertical distribution patterns of total clay below the Mid-Cimmerian Unconformity is shown in Fig. 9.

Excluding Well 21/18-6, no obvious vertical distribution trend of clay (including kaolinite) content toward the unconformity surface is apparent. Although the precipitation of kaolinite is commonly associated with feldspar alteration and dissolution, there is a positive correlation between feldspar and kaolinite only in Well 21/18-6, with a lack of correlation in the other three wells (Fig. 9).

5.3. Mica

Mica is a common component in most of the sandstone samples. Point counting shows marked variation (2%–25%) in the amount of mica below the unconformity surface (Table 7, Fig. 11). However, there is no apparent systematic vertical distribution, and we infer that the variation seen is most likely to be proportional to grain size, which can be related to the depositional process rather than to either the sediment provenance or diagenetic process.

5.4. Porosity values

As mentioned above, there is a difference between porosity values from point counting (1%–15%) and core analysis using helium porosimetry (3%–21%). However, the correlation between measured core porosity (He porosity) and point-counted modal porosity for the four studied wells indicates that both porosity values are more or less closely related (Fig. 12). The greater variation observed from helium porosimetry measurements is due to more measurements having been made, which included a wider range of facies – e.g. more mud-rich facies giving lower porosity values.

Primary intergranular porosity, which exists as pores between framework grains, is very low in the four studied wells. This can be related to many factors, including grain size, sorting and diagenetic

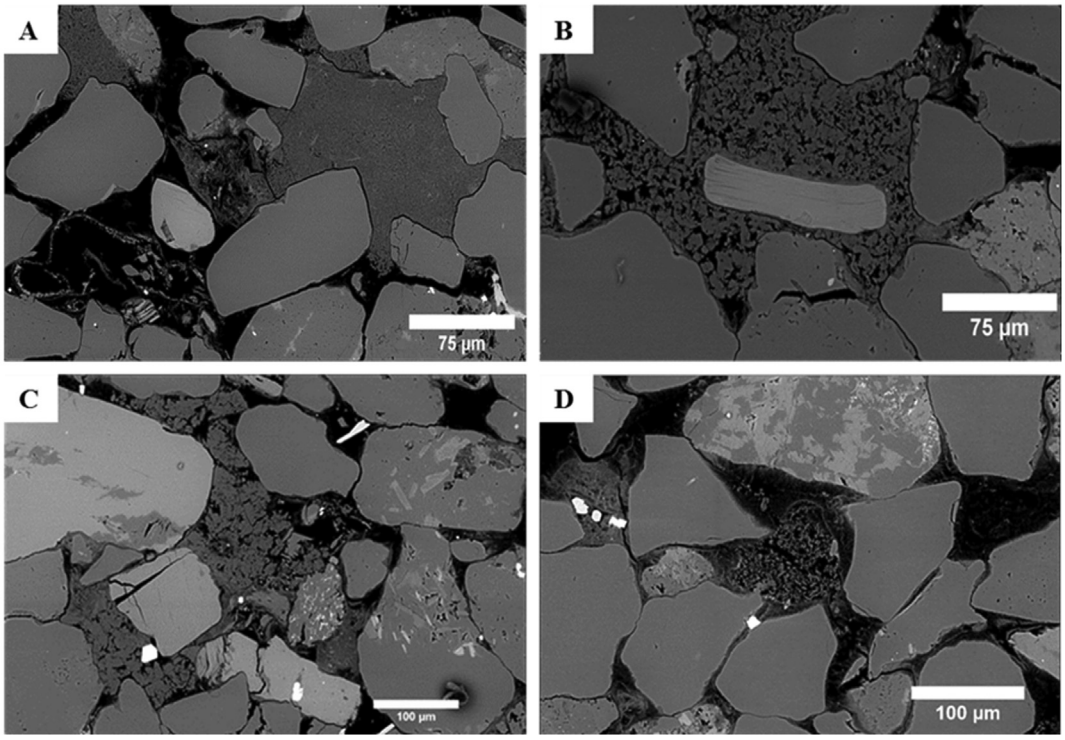

Fig. 10. BSE images showing the various types and distribution of kaolinite below the unconformity surface in Skagerrak sandstone. **A**. Intermixed clay (mainly kaolinite) squeezed between grains filling pore spaces which can be either detrital or early diagenetic kaolinite. Well 21/18-6, depth, 10417 ft (3175.1 m). **B**. and **C**. Regular crystals of kaolinite stacked in "booklets" or vermicular habit, reflecting a late diagenetic product formed in situ due to alteration and replacement of feldspar. Samples are from Wells 21/18-2A, depth 10017.5 ft (3053.3 m) and Well 21/18-6, depth 10417 ft (3175.1 m). **D**. Kaolinite within pore space formed as result of feldspar alteration and dissolution and appearing with a hint of the grain outline. Well 21/18-6, depth 10449.4 ft (3185 m).

Table 7
Petrographic analysis data of mica content below the unconformity surface in Wells 21/18-6, 21/18-2A, 21/18-3 and 21/18-4.

Well 21/18-6		Well 21/18-2A		Well 21/18-3		Well 21/18-4	
MCU at 10415.5 ft		MCU at 10017 ft		MCU at 10332 ft		MCU at 10698.7 ft	
Depth (ft)	Mica %	Depth (ft)	Mica %	Depth (ft)	Mica %	Depth (ft)	Mica %
10415.7	2.8	10017.1	12	10332	8.1	10698.7	8.3
10415.8	2.3	10017.5	5.6	10332.5	7.8	10700.5	24.7
10417	5	10021	6	10333.5	24	10701.8	6
10418.7	2	10023	8.9	10336.5	10.4	10708.5	24.4
10420.2	2.1	10026.5	13	10343.8	17	10714.5	3.7
10424	1.6	10033.8	16	10352.8	15	10724.5	8
10431.2	1	10053.9	4.3	10361	12	10734.1	5.3
10437.3	16.7	10076.9	8	10377.8	13.3	10746.5	3
10449.4	2.1	10111	3.3				

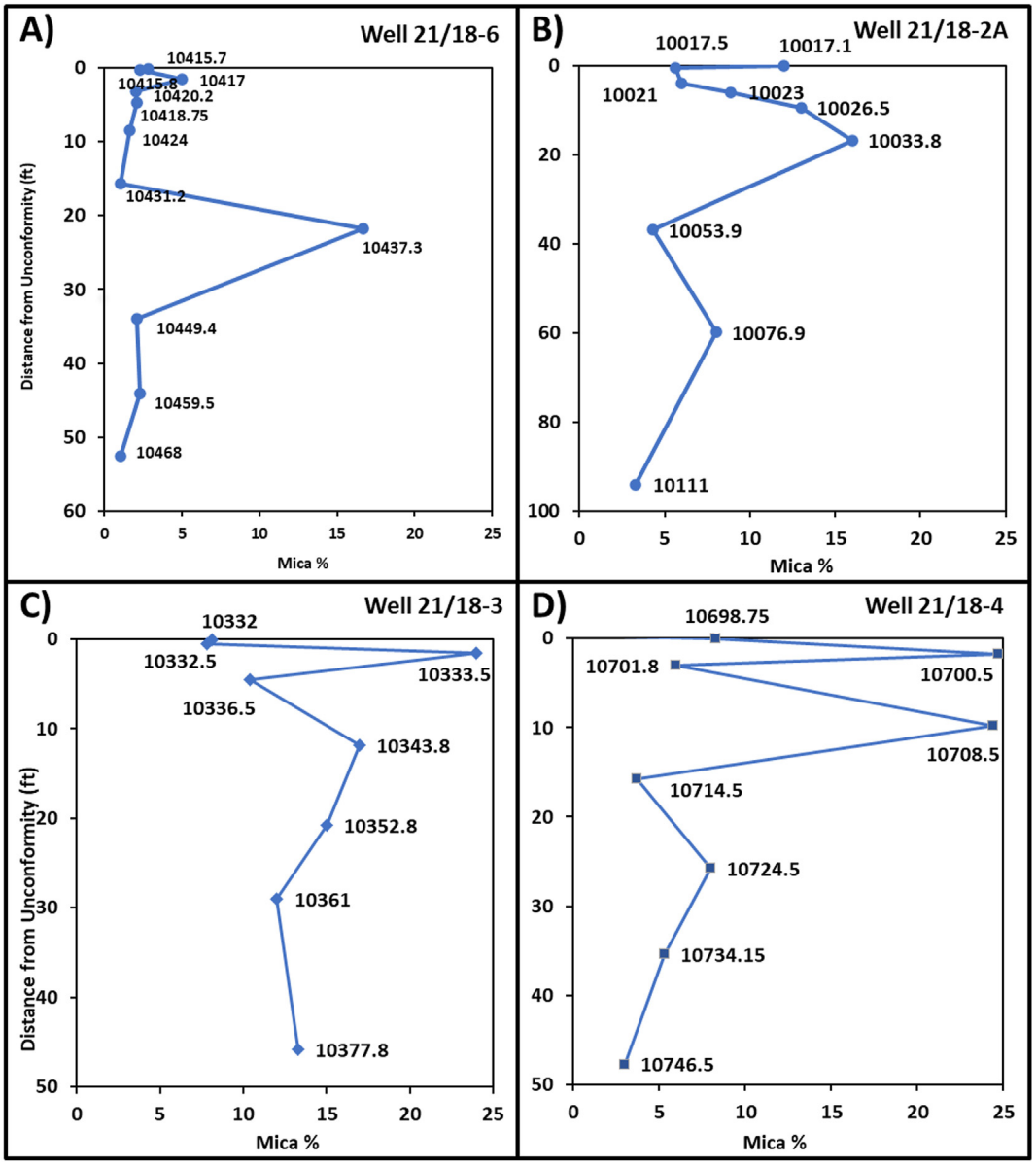

Fig. 11. The vertical distribution patterns of mica below the Mid-Cimmerian Unconformity in the studied wells. (**A**), (**B**), (**C**) and (**D**) show absence of vertical systematic distribution patterns of mica toward the unconformity surface in the four studied wells.

process, as in many cases these pores are filled partially or completely by digenetic carbonate and clay cement. Secondary intragranular porosity, has been formed mainly due to the partial or complete dissolution of detrital grains (commonly feldspar), and

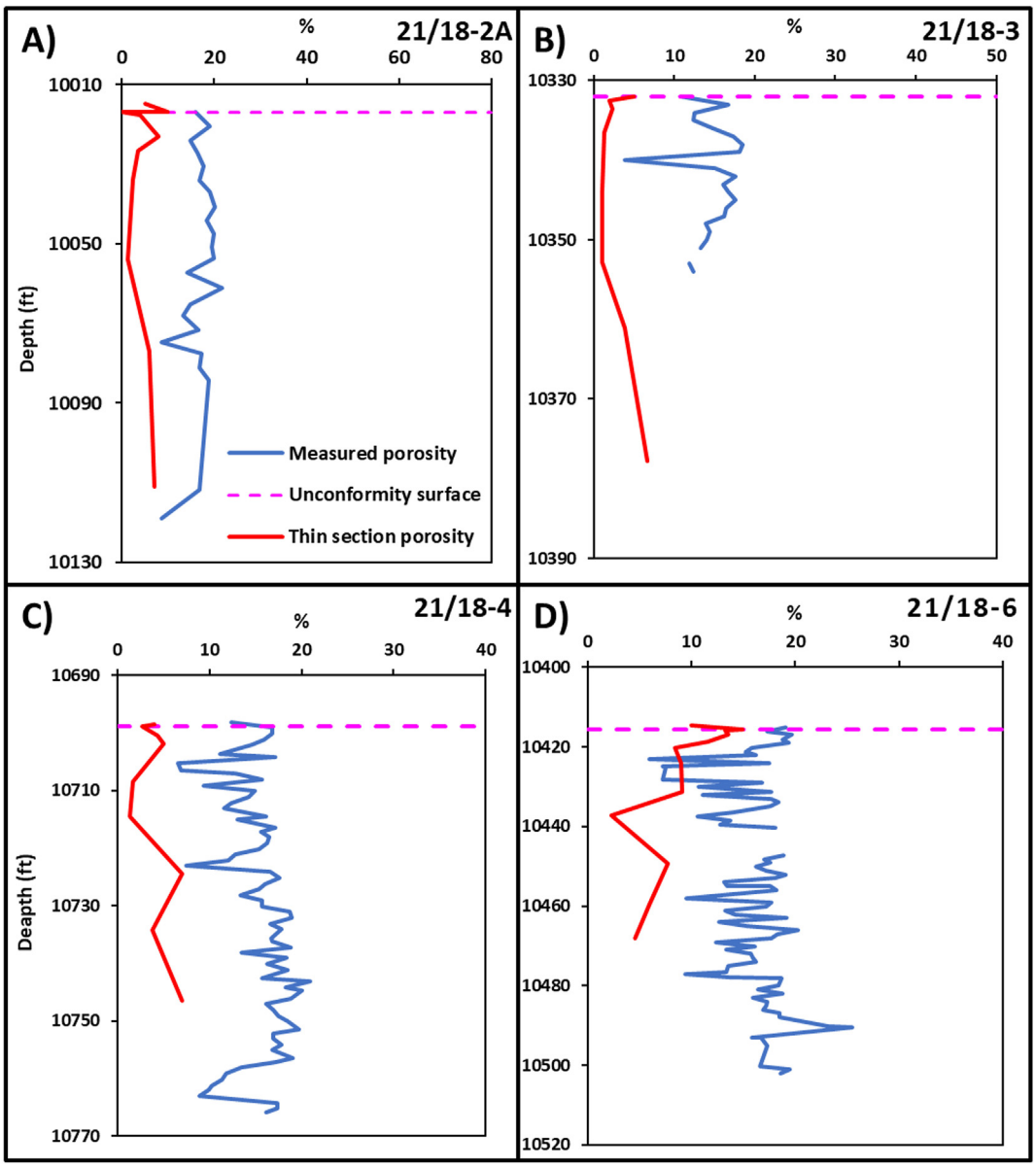

Fig. 12. A correlation between measured core porosity (He porosity) and a visible point counted modal porosity for the four studied wells, (**A**), (**B**), (**C**) and (**D**), indicating that both porosity values are related.

can be referred to as dissolution porosity, which serves to enhance the overall porosity. However, dissolution of feldspar is associated with the formation of clay minerals (mainly kaolinite), which then to reduces porosity. The microporosity is mostly associated with authigenic clays, mainly kaolinite, and with partially dissolved feldspar grains. This type of secondary porosity also enhances total porosity (Table 6).

There is no systematic variation in the amount and vertical distribution of total porosity, including all three types, with respect to the unconformity surface in three out of the four wells. However, in Well 21/18-6, there is a fairly systematic increase in porosity toward the unconformity, from around 4% at 15 feet (4.572 m) below the unconformity surface to around 15% closest to the surface (Table 5). This increase in porosity correlates closely with the reduction in feldspar (Fig. 13), which suggests that dissolution of feldspar is the main cause of enhanced secondary porosity in Well 21/18-6. Although the same relationship between feldspar dissolution and increased secondary porosity is valid for all four wells, the trend towards the unconformity is only seen in the top part of Well 21/18-6. This is possibly because the increase of porosity volume due to mineral dissolution is partly balanced by the generation and precipitation of a similar volume of diagenetic minerals in three out of four wells (Fig. 13).

6. Discussion

6.1. Origin and timing of dissolution and production of secondary porosity

Our petrographic analysis shows that secondary porosity in the Skagerrak Formation sandstones is mainly due to the partial or complete dissolution of feldspar grains. This represents an important part of the overall porosity and reservoir quality. Here, we consider the nature and timing of five different scenarios that may

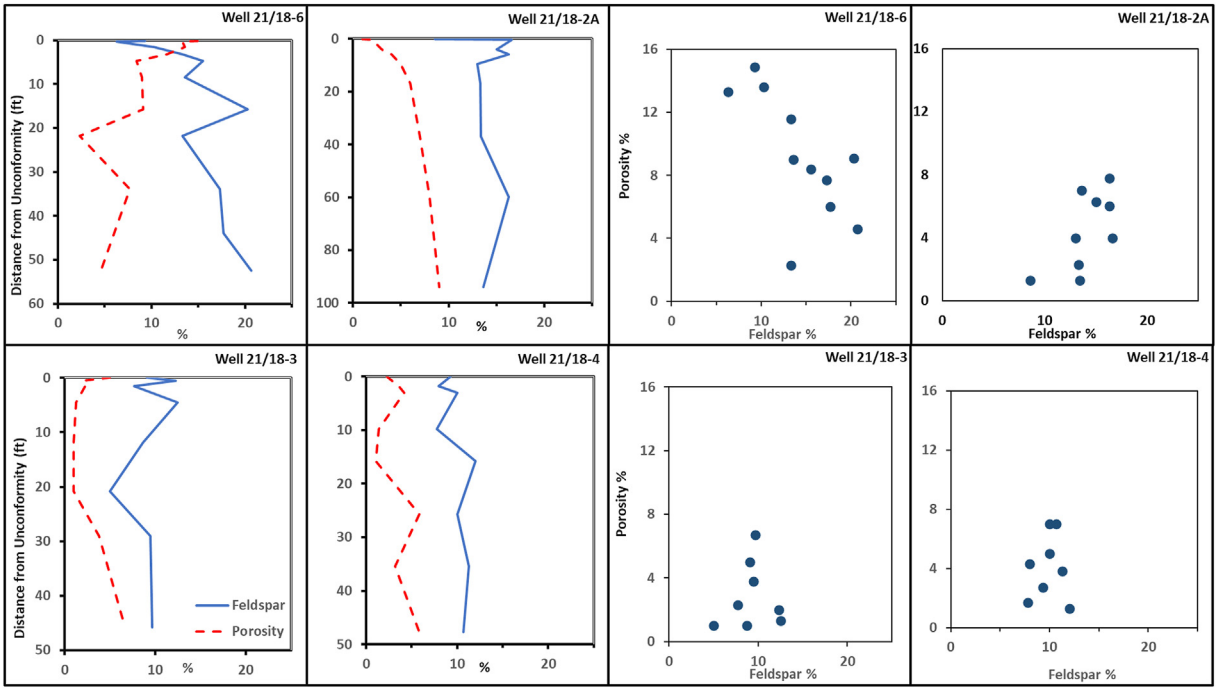

Fig. 13. The distribution of porosity and feldspar below the unconformity surface in the four studied wells (four panels on left). Well 21/18-6 shows possible correlation between porosity and feldspar until depth 10429 ft (3178.8 m). The other wells (21/18-2A, 21/18-3 and 21/18-4) show no clear correlation between the distribution of porosity and feldspar. Scatter plots (four panels on right) show lack of correlation between porosity content and feldspar, except in Well 21/18-6.

have caused such dissolution.

6.1.1. Early-stage meteoric water

This scenario attributes the dissolution of feldspar grains to the early influx of meteoric water shortly after the deposition of the Skagerrak sandstone sediments. Mildly acidic meteoric water may have been able to penetrate the sediments after their deposition and burial, leading to the dissolution of unstable minerals and enhancement of porosity. However, the ability of this water to leach and dissolve minerals would be limited and show a marked decrease with depth, because meteoric water when starting to penetrate is undersaturated, and then rapidly becomes saturated following mineral interaction (Bjorlykke and Aagaard, 1992).

There are several reasons why we believe that an early-stage meteoric influx was *not* the primary factor involved:

(a) The late Triassic climate was semi-arid, in which case meteoric water influx would have been limited (Ketzer et al., 2009), and yet feldspar dissolution is very widespread throughout the Skagerrak Formation.
(b) If the dissolution occurred directly after deposition, secondary pores formed by the dissolution of feldspar grains would most likely be destroyed by compaction, whereas we observe oversized pores that are almost the same size as the surrounding framework grains. These oversized pores have not been affected by compaction, despite the present depth of burial in excess of 3000 m and the presence of other signs of sediment compaction (Fig. 14 A and B).
(c) In most cases, parts of the dissolved feldspar grains had been replaced by kaolinite. The generated kaolinite was within the secondary pore space and associated with microporosity, indicating no signs of compaction (Fig. 14C and D).
(d) In other cases, parts of the original feldspars have been replaced by albite. These albite replacements maintain the original shape of the grain. As albite commonly dissolves faster than feldspar grains (Bjorkum et al., 1990), this indicates that these patches of albite were most likely to be formed after the feldspar dissolution, which therefore must have taken place in deep burial, post-dating compaction (Fig. 14).

6.1.2. Early-stage marine incursion event

This scenario attributes diagenetic changes to the early stage marine incursion over the continental Skagerrak Formation sandstone across the unconformity surface. This was a significant event early in the geological history of the region, and is likely, therefore, to have had some effect on the underlying section. The Ca-rich seawater might have induced some calcite cementation, together with possible dissolution of feldspar grains or other unstable minerals, leading to an enhancement of porosity locally. The apparent leaching of red colouration from the upper part of the Skagerrak Formation may have occurred as a result of this event.

However, there are several reasons why we believe that an early-stage marine influx was *not* the primary factor involved in the development of secondary porosity:

(a) There is no evidence for enhanced calcite cementation in the Skagerrak sandstones directly linked to the unconformity surface. Calcite cementation does occur in about 50% of the samples studied, some of which is interpreted as early-stage and some late-stage. It is possible that some of the early-stage calcite cementation was subsequently removed by dissolution, perhaps by late-stage meteoric waters (6.1.3 below) or by deep-burial organic acids (6.1.4, 6.1.5). However, there is no clear evidence for this process, and none links it to the unconformity surface. We do not exclude the possibility of some additional secondary porosity after calcite dissolution.

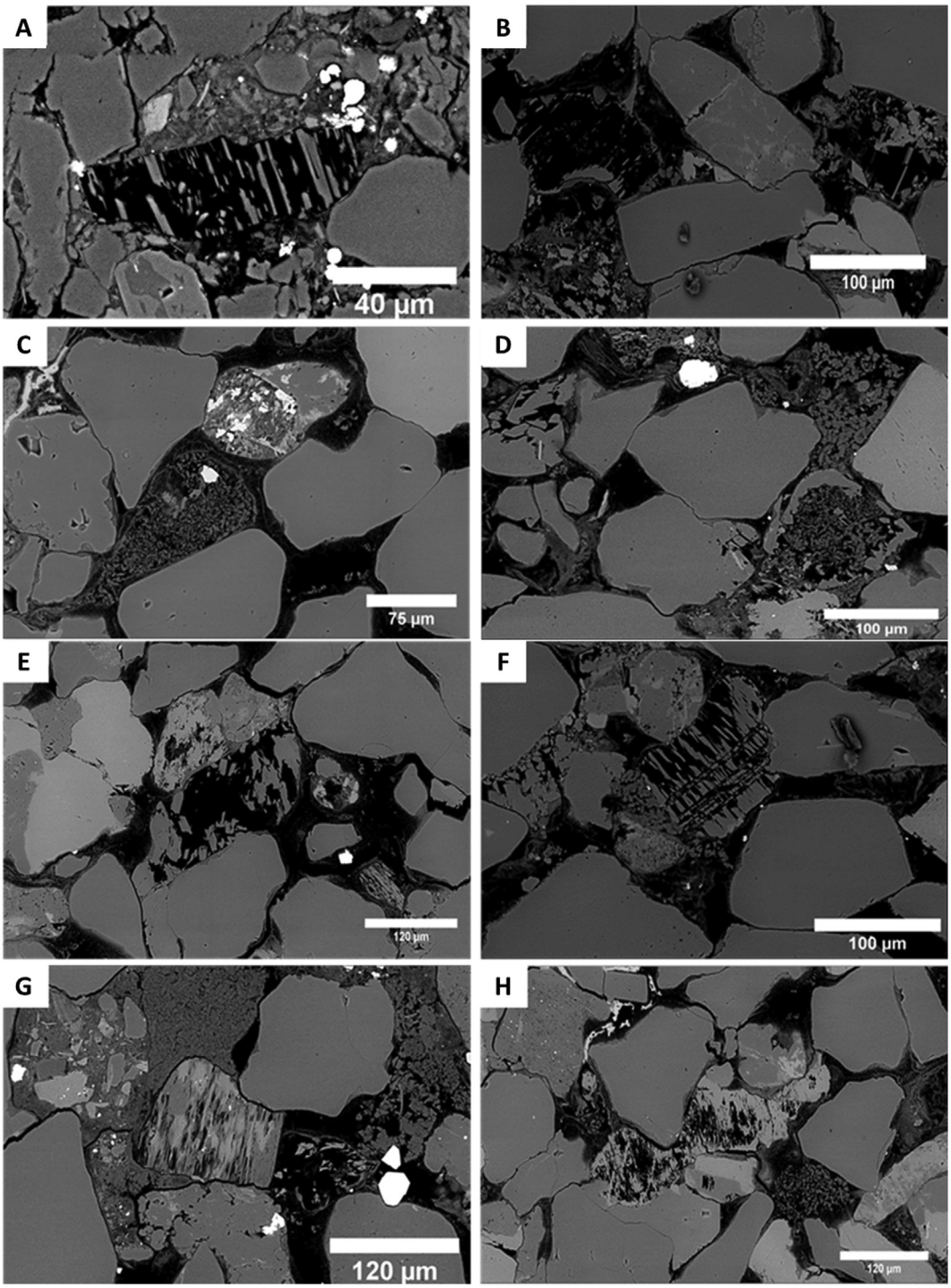

Fig. 14. Backscattered electron images: **A** and **B** show that dissolution of feldspar grains produced oversized pores almost the same size as the other surrounding framework grains, with no signs of compaction, despite the depth of more than 3300 m, Well 21/18-3, 10332 ft (3149.1 m) and Well 21/18-2A, 10017.5 ft (3053.3 m) respectively. **C** and **D** indicate formation of kaolinite within the pore space and associated with microporosity and indicating no signs of compaction, despite the depth of sandstone burial which is in excess of 3000 m, Well 21/18-6, 10449.4 ft (3185 m) and 10417 ft (3175.1 m), respectively. **E** and **F** show partial to complete dissolution of feldspar grains with the preservation of the shape of the feldspar grains with no compaction signs, despite the depth of more than 3300 m: Well 21/18-6, 10449.4 ft (3185 m) and Well 21/18-2A, 10017.5 ft (3053.3 m), respectively. **G** and **H** show authigenic albite in corroded feldspar grain associated with microporosity and indicating no signs of compaction, despite the depth of sandstone burial, which exceeds 3000 m: Well 21/18-6, 10449.4 ft (3185 m).

(b) The mildly alkaline nature of marine waters would be unlikely to affect any marked dissolution of feldspar grains or other unstable minerals. The dissolution of these are the primary cause for secondary porosity development according to the present study.

(c) However, even if there had been some early dissolution of feldspar grains related to marine water, these would most likely be destroyed by the subsequent compaction to the present depth of burial in excess of 3000 m. Likewise, the

kaolinite found replacing some of the dissolved feldspars shows no signs of compaction.

(d) For other evidence that mitigates against this scenario, see discussion below (6.1.3).

6.1.3. Late-stage meteoric water

This scenario attributes the dissolution of feldspar grains to the late influx of meteoric water following uplift and erosion resulting from the Cimmerian orogeny. Uplift of the Western Platform in the central North Sea during the Lower to Middle Jurassic resulted in erosion and removal of the Early and Mid-Jurassic sandstones and development of the Mid-Cimmerian Unconformity (also known as the Intra-Aalenian Unconformity), which lies directly above the Skagerrak Formation in the area of interest.

Petrographic analysis has shown much evidence for the late dissolution of feldspar grains and the creation of secondary pores in most of the analysed samples. In many cases, the original shape of the partly or completely dissolved feldspar grains has been preserved by a remnant chlorite grain coating, which indicates that the dissolution of feldspar grains is most likely to have occurred in a late diagenesis stage, after the chlorite coating was precipitated. These authigenic chlorite grain coats were likely formed during an early to mid-diagenetic phase as a result of replacement of other clay minerals such as smectite and kaolinite, or due to dissolution and re-precipitation of syn-depositional chlorite (Stricker and Jones, 2016). This late dissolution of feldspar grains led to the creation of secondary pores and therefore enhanced the total porosity of the Skagerrak Formation. However, in many cases the dissolution of feldspar grain was associated with the precipitation of pore filling kaolinite and/or illite (fibrous pore-lining diagenetic illite) which would lead to a relative decrease in the total porosity of Skagerrak sandstone.

There are several lines of evidence why we believe that late-stage meteoric water influx related to the unconformity surface was *not* the primary factor involved:

(a) There is no systematic decrease of feldspar volume and corresponding increase in porosity toward the unconformity surface over a relatively thick interval. The thickness of pervasive late diagenetic influence of meteoric waters below unconformity surfaces typically varies between ten to hundreds of metres, and any changes are expected to occur systematically over this interval toward the unconformity surface (Shanmugam, 1988). However, our results show no significant systematic vertical variation in the volume and distribution of either feldspar or total porosity, including secondary porosity, toward the unconformity surface for three of four wells. In the one well in which feldspar and porosity values do vary systematically, this only affects the first 15 ft (4.572 m). This difference between wells can be interpreted as due to differential rates or amounts of erosion of the Skagerrak sandstones. If there was a slower rate and less erosion in the area of Well 21/18-6, then the longer time of exposure at the surface may have led to a greater effect (i.e. more dissolution) in this well than the others.

(b) There is no sign of any partial destruction of secondary pores due to the post-unconformity compaction processes. Even if the uplifted sediments were already partially cemented, their maximum burial prior to uplift was no more than about 100 m. It is, therefore, most likely that meteoric weathering and feldspar dissolution followed by burial to depths in excess of 3000 m, would have caused significant disruption to the secondary pores. Instead, the usually delicate dissolution structures remain completely intact (Fig. 14).

(c) The absence of any systematic increase of kaolinite volume toward the unconformity surface indicates that most of the observed kaolinite was formed in situ and related to late diagenetic processes. This is supported by the observed delicate euhedral booklets in most samples and the high microporosity within the kaolinite crystals. No obvious vertical distribution trend of clay (kaolinite) content toward the unconformity surface is observed, whereas, if the creation of these kaolinites was related to an influx of meteoric waters through the Mid-Cimmerian Unconformity, systematic vertical change toward the unconformity surface would be expected.

(d) There is clear evidence for mechanical compaction in many samples, including bending of mica grains, squeezed clay cement between grains, grain contact dissolution with sutured contacts and grain fracturing. Yet, these features coexist with the presence of oversized secondary pores, which are associated with in situ diagenetic kaolinite with microporosity. These secondary pores, which are approximately the same size as the surrounding framework grains and generated as a result of feldspar dissolution do not show any signs of compaction, despite the great depth of burial. The presence of compaction features and uncompacted pores and highly microporous kaolinite within the same field of view within one sample (Fig. 15) indicates that the dissolution of feldspar grains and the formation of kaolinite were most likely to have occurred after mechanical compaction had occurred. These observations mitigate against both early and late-stage meteoric influx scenarios.

It could, of course, be argued that the observed compaction signs may have been formed as a result of a compaction process that occurred before the creation of the unconformity surface. This hypothesis can be disproved by the knowledge that the maximum thickness of deposition above the Skagerrak Formation, before Cimmerian uplift occurred, does not exceed 100 m. This thickness of sedimentary cover would not cause the observed signs of compaction and, most probably, only the initial phase of compaction would have taken place.

Some further considerations regarding the likely burial depth at which feldspar dissolution took place are as follows.

Quartz cementation: Is it possible that an abundant quartz cement caused compaction resistance, therefore preserving the oversized secondary pores? However, this can be discounted as: (a) quartz cement rarely forms in abundance at a depth range of 1.5–2 km (Dillon et al., 2004), but requires relatively deep burial to temperatures above 70–80 °C (Harwood et al., 2013); (b) such burial depths were not reached in the study area prior to the Cimmerian uplift; and (c) there is no evidence of abundant of quartz overgrowths in any of the samples studied.

Overpressure: Is it possible that fluid overpressure caused compaction resistance? However, this is also discounted as on the basis of downhole pressure data, from the repeat formation tester for the Kittiwake Field. Both reservoir formations (Fulmar Formation and Skagerrak Formation) have a similar pressure, which indicates full fluid communication throughout the field. Formation overpressure was most likely to have been developed at a burial depth of 3 km (Wilkinson et al., 2014), so that it would not have inhibited compaction of other diagenetic changes. Moreover, according to Stricker and Jones (2016) there would be almost no effect on compaction if overpressure occurred at depths greater than 2500 m.

Therefore, it seems that whether compaction was resisted by an abundant quartz overgrowth or by the development of overpressure, the dissolution of feldspar grains and creation of

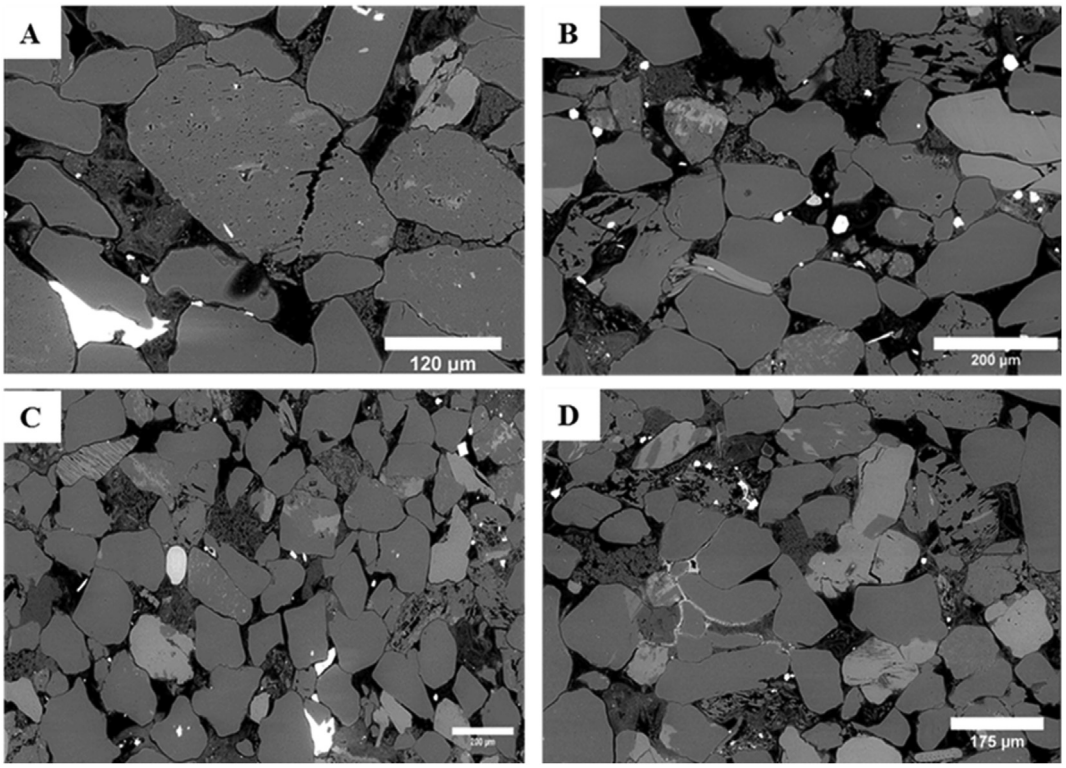

Fig. 15. Backscattered electron images: A, B, C and D show characteristics of compaction state (such as bending of mica grains, squeezed clay cement between grains, grain contact dissolution with sutured contacts and grain fracturing) and uncompacted pores and highly microporous kaolinite within the same field of view of one sample.

secondary pores, which in many cases were associated with booklets of the highly microporous in-situ kaolinite within the Skagerrak Formation sandstones, were unlikely to have been formed as a result of the influx of meteoric waters through the Mid-Cimmerian Unconformity and most likely to have been formed at a burial depth of not less than 2 km.

Rate of erosion: Uplifted and exposed sedimentary rocks that have been subjected to meteoric waters are prone to erosion, and the rate of this erosion depends on many factors, including the properties of the exposed material, topography and climate of the area. Therefore, it is important to bear in mind that the expected effect of meteoric water on the exposed sedimentary rocks will be only preserved if the rate of erosion was less than the rate of meteoric water penetration and alteration, otherwise, any diagenetic effect of these waters (e.g. dissolution or kaolinization of minerals) will be removed by erosion (Bjorkum et al., 1990). Hence, it is possible that the rate of erosion of the Skagerrak sandstones underlying the Mid-Cimmerian Unconformity was higher than the rate of meteoric water penetration and, therefore, there was no relationship between the observed diagenetic products and the formation of the Mid-Cimmerian Unconformity.

6.1.4. Thermal organic acids

This scenario attributes the dissolution of unstable minerals (mainly feldspars) to the influx of organic acids and/or CO_2 produced by thermal maturation of organic matter. The Kimmeridge Clay source rocks of Late Jurassic age are thick, deeply buried and highly mature in the vicinity of the Kittiwake Field, and the oil charge would have most likely been preceded by an influx of (highly) acidic fluids.

In addition, this study provides clear evidence that the dissolution of feldspar grains post-dates the majority of the mechanical compaction and that secondary porosity has been largely protected from any further diagenetic processes. Moreover, it is also clear that in many cases the increase of porosity due to feldspar grain dissolution was not associated with precipitation of reaction products (such as kaolinite, illite etc.) This may indicate that the reaction products resulting from the dissolution of grains were removed from the sandstones and transported to other places by pore fluid flow while the sandstone formation was becoming overpressured. This removal of reaction products would lead to higher porosity and must have been occurring in an open system with continued pore fluid migration. From all of these considerations, it is most likely that the observed late generation of secondary porosity was preserved by the infill of hydrocarbons in highly overpressured sandstone. This secondary porosity would have been created by an aggressive fluid influx, which was possibly generated from the Kimmeridge Clay Formation.

6.1.5. Bio-organic acids

This scenario attributes the dissolution of unstable minerals to the influx of organic acids and CO_2 produced by in situ oil biodegradation. Biodegradation of oil as a result of bacterial metabolism in the reservoir is usually associated with an increase of hydrocarbon acidity, and the generation of organic acids and CO_2 (Ehrenberg and Jakobsen, 2001). In subsurface reservoirs, most oil biodegradation processes occur within the transition zone (across the oil-water contact, OWC), as within this area the chemical interaction of hydrocarbon with water and minerals leads to the generation of organic acids and CO_2 in the reservoir, similarly to the creation of organic acids and CO_2 from the source rocks (Head et al., 2003).

In the Kittiwake Field, the OWC transition zone is at about 10430 ft (3179.06 m) TVSS. The samples analysed from three of the four wells were taken from significantly above or below the transition zone. However, those from Well 21/18-6 were taken from

10,415 to 10,468 feet (3174.4–3190.6 m) depth, and so actually span the transition zone. It is noteworthy that this is the only well showing correlation between the dissolution of feldspar and the creation of secondary porosity toward the unconformity surface. The depth of the unconformity surface in this well is at 10415.5 feet (3174.6 m), whereas the depth of the OWC is around 10430 feet (3179.06 m). This 15 feet (4.572 m) difference is exactly the thickness over which there is a systematic trend in the amounts of porosity and feldspar toward the unconformity surface.

While this observation is not conclusive evidence, it nevertheless supports the oil biodegradation hypothesis.

6.2. Origin and timing of kaolinization

Kaolinite is common in all the studied wells of the Skagerrak sandstones. It generally occurs: (a) in association with other clay minerals (such as illite), where it could be either detrital or diagenetic in origin (Fig. 10 A); and (b) in well-developed crystals stacked in booklets filling pore spaces, where it is most likely of diagenetic origin (Fig. 10 B and C), in some cases with the remnant hint of the original grain outline (Fig. 10 D). Although most of the kaolinite is interpreted to have been formed as a result of alteration and replacement of feldspar grains, the increase in the amount of kaolinite is not associated with a decrease in feldspar content, with the exception of Well 21/18-6, which showed some correlation (Fig. 9). This overall lack of correlation can be related to: (a) an initial variability in the amount of feldspar within the sandstones; (b) the alteration and kaolinization of other minerals, such as micas and silicate rock fragments, in addition to feldspars; and (c) the influx of fluids from outside the area with the necessary chemical composition (and high silica content) to facilitate kaolinization.

The evidence that most of the kaolinite present was formed in situ and related to late diagenetic processes, includes: (a) the vermicular textures and delicate euhedral booklets observed in most samples; (b) the growth of kaolinite between pre-existing sheets of (detrital) mica; (c) the common presence of oversized secondary pores containing kaolinite; (d) the high microporosity within kaolinite patches, with no signs of compaction; and (e) the absence of a systematic increase of kaolinite volume toward the unconformity surface.

If the formation of kaolinite was related to the influx of meteoric waters through the Mid-Cimmerian Unconformity, systematic vertical change (i.e. an increase in kaolinite) toward the unconformity surface would be expected. This is not the case and, in fact, both an increase and decrease is seen over short distances in different wells. It seems most likely, therefore, that kaolinization of the Skagerrak sandstone took place as a late-stage diagenetic process at the same time as feldspar dissolution and related to the same influx of organic acids and carbon dioxide.

7. Conclusion

Detailed petrographic analysis of the reservoir sandstone from four wells in the Skagerrak Formation of the Kittiwake Field of the North Sea, which directly underlies the Mid-Cimmerian Unconformity, was carried out in order to assess the role of this unconformity on reservoir quality. The principal findings are:

- Secondary porosity development is common, and demonstrated by: the presence of oversized pores, the partial and complete dissolution of detrital grains, corroded grain margins, remnant grain margins with diagenetic clay filling.
- This porosity developed from the post-depositional dissolution of unstable silicate minerals, primarily feldspars, and as a microporosity within the diagenetic kaolinite pore filling.
- Dissolution post-dated most of the mechanical compaction and/or was protected from any further diagenesis process, despite burial to present depths greater than 3300 m. Evidence includes: the vermicular texture and delicate euhedral booklets of kaolinite, the growth of kaolinite between the pre-existing sheets of mica, and common oversized secondary pores, some containing kaolinite.

We therefore conclude that there is *no evidence* to suggest the cause of feldspar dissolution and porosity development is related to the presence of the Mid-Cimmerian unconformity. By contrast, evidence against any effect of the unconformity includes: (a) the absence of a systematic decrease of feldspar volume and increase of secondary porosity toward the unconformity surface; (b) the absence of a systematic increase in kaolinite volume toward the unconformity surface; and (c) the absence of any compaction effects on the oversized pores, delicate remnant pore rims and kaolinite filling.

Furthermore, there is no evidence for leaching or cementation linked to meteoric water influx either shortly after deposition or following the uplift and exposure that led to development of the Mid-Cimmerian Unconformity. Instead, we propose that the dissolution of feldspar and generation of secondary porosity were the result of late-stage diagenetic processes. These are most likely related to the influx of organic acids and carbon dioxide generated either from thermogenic maturation of the Kimmeridge Clay source rock, or from biodegradation of oil within the reservoir, particularly at the transition zone near the oil-water contact.

Declaration of competing interest

The authors declare that there is no conflict of interest.

Acknowledgements

We gratefully acknowledge to The Department of Earth Science at Elmergib University (Libya) for providing all necessary administrative support throughout. AA offers his special gratitude to Prof. Dorrik Stow, Dr. Helen Lever and Dr. Zeinab Smillie, who provided a great support from Heriot-Watt University. The British Geological Survey is thanked for supplying all samples. A big thank to Dr. Jim Buckman (Heriot Watt University) who provided assistance with SEM imaging.

References

Bjorkum, P.A., Mjos, R., Walderhaug, O., Hurst, A., 1990. The role of the late Cimmerian unconformity for the distribution of kaolinite in the Gullfaks Field, northern North Sea. Sedimentology 37 (3), 395–406.
Bjorlykke, K., Aagaard, P., 1992. Clay Minerals in North Sea Sandstones.
Buckman, J., 2014. Use of automated image acquisition and stitching in scanning electron microscopy: imaging of large scale areas of materials at high resolution. Microsc. Anal. 28, 13–15.
Dillon, C.G., Worden, R.H., Barclay, S.A., 2004. Simulations of the effects of diagenesis on the evolution of sandstone porosity. J. Sediment. Res. 74 (6), 877–888.
Ehrenberg, S., Jakobsen, K., 2001. Plagioclase dissolution related to biodegradation of oil in brent Group sandstones (Middle Jurassic) of Gullfaks field, northern North Sea. Sedimentology 48 (4), 703–721.
Glennie, K.W., Armstrong, L., 1991. The Kittiwake field, block 21/18, UK North Sea. Geological Society, London, Memoirs 14 (1), 339–345.
Glennie, K.W., 1998. Petroleum Geology of the North Sea: Basic Concepts and Recent Advances. Blackwell Publishing, Oxford.
Harwood, J., Aplin, A.C., Fialips, C.I., Iliffe, J.E., Kozdon, R., Ushikubo, T., Valley, J.W., 2013. Quartz cementation history of sandstones revealed by high-resolution SIMS oxygen isotope analysis. J. Sediment. Res. 83 (7), 522–530.
Head, I.M., Jones, D.M., Larter, S.R., 2003. Biological activity in the deep subsurface and the origin of heavy oil. Nature 426, 344–346.
Ketzer, J., Morad, S., Nystuen, J., De Ros, L., 2009. The role of the cimmerian unconformity (early cretaceous) in the kaolinization and related reservoir-quality evolution in triassic sandstones of the snorre field, North Sea. Clay

Miner.Cements Sandstones IAS Special Publication 34 (19), 361–382.
Pettijohn, F.J., Potter, P.E., Siever, R., 1972. Sand and Sandstone. Springer-Verlag, Berlin.
Rittenhouse, G., 1972. Stratigraphic-Trap Classification: Geologic Exploration Methods.
Shanmugam, G., 1988. Origin, Recognition, and Importance of Erosional Unconformities in Sedimentary Basins. New Perspectives in Basin Analysis. Springer, New York, pp. 83–108. K. Kleinspehn and C. Paola.
Stricker, S., Jones, S.J., 2016. Enhanced Porosity Preservation by Pore Fluid Overpressure and Chlorite Grain Coatings in the Triassic Skagerrak, Central Graben, vol. 435. Special Publications, North Sea, UK. Geological Society, London. SP435. 434.
Wakefield, L.L., Droste, H., Giles, M.R., Janssen, R., 1993. Late Jurassic Plays along the Western Margin of the Central Graben. Geological Society, London, Petroleum Geology Conference series.
Wilkinson, M., Haszeldine, R.S., Morton, A., Fallick, A.E., 2014. Deep burial dissolution of K-feldspars in a fluvial sandstone, pentland formation, UK Central North sea. J. Geol. Soc. 171 (5), 635–647.
Wu, K., Paton, D., Zha, M., 2013. Unconformity structures controlling stratigraphic reservoirs in the north-west margin of Junggar basin, North-west China. Front. Earth Sci. 7 (1), 55–64.